THE JOURNAL OF COMPARATIVE NEUROLOGY 340:65–86 (1994)

Identification and Visuotopic Organization of Areas PO and POd in *Cebus* Monkey

SERGIO NEUENSCHWANDER, RICARDO GATTASS, AGLAI P.B. SOUSA, AND MARIA CARMEN G.P. PIÑON
Instituto de Biofísica Carlos Chagas Filho, Universidade Federal do Rio de Janeiro, RJ 21941-900 Brasil

ABSTRACT

Two visual areas of the anterior bank of the parietooccipital sulcus, areas PO and POd, were identified and their visual field representations were studied in six anesthetized and paralyzed *Cebus* monkeys. The definition of these areas was based on electrophysiological mapping and myeloarchitecture. PO is located in the ventral aspect of the anterior bank of the parietooccipital sulcus and ventral precuneate gyrus. It borders area V2 posteriorly and ventrally in the depth of the parietooccipital sulcus, area V3d laterally, and another undescribed visual area medially. POd was located dorsal to area PO and ventral to architectonic area PE. The representations of the visual field in areas PO and POd are complex. In each hemisphere, these areas have a virtually complete representation of the contralateral visual hemifield. Different from the previously described visual areas, in PO and POd there is a precise organization of isopolar lines and a complex organization of the isoeccentric ones. In PO, as well as in POd, the representation of the horizontal meridian runs dorsoventrally along the parietooccipital sulcus. The upper visual quadrant is represented medially and the lower visual quadrant laterally. A large and complex representation of the periphery, from 20° to 60° eccentricity is present at the lateral and medial portions of these areas. By contrast, the representation of the central 20° is very small in both PO and POd. The central visual field is represented ventrally in PO and dorsally in area POd. Area POd shows a more stratified myeloarchitectonic pattern than PO and both areas can be distinguished from other surrounding areas by their heavier myelinated pattern.

Key words: prestriate cortex, visual topography, parietal cortex, receptive fields, myeloarchitecture

Electrophysiological methods have been used successfully to identify new visual areas and describe their visual topography. (Daniel and Whitteridge, '61; Allman and Kaas, '71, '74, '76; Gattass et al., '87; Rosa et al., '88; Fiorani et al., '89; Boussaoud, '91). In nonhuman primates, areas V1, V2, V3, V4, and MT were defined as visual areas containing partial or complete representations of the contralateral visual field in New and Old World monkeys (Daniel and Whitteridge, '61; Allman and Kaas, '71, '74; Gattass and Gross, '81; Gattass et al., '81, '87; Rosa et al., '88, Fiorani et al., '89). These visual areas have different degrees of precision in their representations of the visual field. Receptive field size and scatter in position at a given eccentricity increase in more anteriorly located visual areas (Gattass et al., '86). In *Macaca*, area PO, which borders V2 in the ventral portion of the parietooccipital cleft, has been proposed to be homologous to area M of *Aotus* (Covey et al., '82). In *Aotus*, the medial visual area M is located within cytoarchitectonic area 19 and has a complete representation of the contralateral visual field, with little emphasis on the representation of central vision. Area M borders area V2 posteriorly and shares with this area part of the representation of the horizontal meridian. In *Macaca*, area PO has a similar relationship with V2 and shares as well part of the representation of the horizontal meridian with this area (Covey et al., '82). Area PO, as described by Covey and collaborators ('82), is included within cytoarchitectonic area OA described by Von Bonin and Bailey ('47). In a later review, these authors proposed that the anterior bank of the parietooccipital sulcus may be composed of more than one visual area (Gattass et al., '86). The study of the connections of the anterior bank of the parietooccipital sulcus in the macaque revealed that area PO was located ventrally in the anterior bank and that it receives projections from the peripheral representations of V1 and V2 (Colby et al., '88).

Accepted August 12, 1993.

Address reprint requests to Dr. Ricardo Gattass, Departamento de Neurobiologia, Instituto de Biofísica Carlos Chagas Filho, Bl. G, CCS, Ilha do Fundão, Rio de Janeiro, RJ 21941-900 Brasil.

We have been studying the visual areas in a diurnal New World monkey, *Cebus apella* (Gattass et al., '87; Rosa et al., '88; Fiorani et al., '89), which is similar to *Macaca fascicularis* in brain size, sulcal pattern, and certain aspects of visual behavior (Freese and Oppenheimer, '81). In an attempt to define new visual areas we studied the representation of the visual field in the cortex located in the anterior bank of the parietooccipital sulcus in the *Cebus* monkey. In this paper we report the visual topography of areas PO and POd on the basis of recordings from small groups of neurons and examine the myeloarchitectonic distinctions with other visual areas. Previous descriptions of these data have appeared elsewhere (Neuenschwander, '89; Neuenschwander et al., '90).

MATERIALS AND METHODS

Six *Cebus apella* monkeys weighing between 2.5 and 4.0 kg were used. The cortex of the anterior bank of the parietooccipital sulcus and vicinities was systematically explored by either vertical or oblique electrode penetrations. The visual field representation was determined by relating the location of receptive fields of small clusters of neurons to the recording sites in the cortex.

The preanesthetic medication, induction and maintenance of anesthesia, immobilization, and electrode characteristics have all been described in detail previously (Gattass and Gross, '81). Briefly, prior to the first recording session a chamber and a bolt for holding the head were implanted under aseptic conditions, after the administration of Ketamine hydrochloride (Ketalar; Park Davis; 50 mg/kg) and a benzodiazepinic (Valium; Roche; 2 mg/kg). During the recording sessions, the animals were maintained under nitrous oxide and oxygen (7:3) and immobilized with pancuronium bromide. Varnish-coated tungsten microelectrodes with impedance of about 0.5 MΩ at 500 Hz were used. A single electrode was used in all recording sessions for each animal. Vertical or oblique penetrations were made through the intact duramater. They were spaced by 1.0–1.5 mm, forming a grid encompassing areas PO and POd and adjacent areas. In each penetration, recording sites were separated by 300–500 μm. Electrolytic lesions were made at several sites along each penetration. Visual responses were elicited, under photopic illumination, by white and colored opaque stimuli presented onto a transparent plastic hemisphere located 57 cm from the eye. The eye was focused at 57 cm by means of an appropriate contact lens (see Gattass and Gross, '81, for additional details). The histological procedures were similar to those previously described (Gattass et al., '87). Alternate 40 μm frozen sections, cut either in the coronal or in the parasagittal plane, were stained for cell bodies with cresyl violet or for myelin with a modified Heidenhain-Woelcke method (Gattass and Gross, '81).

Abbreviations

ca	calcarine fissure
HM	horizontal meridian
ip	intraparietal sulcus
lu	lunate sulcus
PEc	cytoarchitectonic area PEc
po	parietooccipital sulcus
pom	medial parietooccipital sulcus
PO	visual area PO
POd	visual area POd
POm	visual area POm
t	transitional myeloarchitectonic area of PO and POd
ts	superior temporal sulcus
V1	primary visual area
V2	second visual area
V3d	third visual area: dorsal
V3v	third visual area: ventral
VM	vertical meridian

Determination of the borders of areas PO and POd

In order to draw the complete perimeter of areas PO and POd, we studied the correspondence between electrophysiological and myeloarchitectonic transitions. The myeloarchitectonic transitions that coincided with reversals of receptive field progressions were then used to delimit areas PO and POd. In each section myeloarchitectonic transitions usually had an uncertainty of 0.5–1 mm, and the borders were drawn in the center of these transitions. The distance between recording sites, the large overlap of receptive fields and the scatter in the location of the receptive field centers in PO and POd determined the precision of the electrophysiological method, which was about 1 mm.

Unfolding the visual cortex

In order to obtain a bidimensional map of the visual topography of areas PO and POd for each animal, we built three-dimensional wire models of layer IV from sections at 7.5 × magnification and then unfolded them, following the same procedure described by Gattass et al. ('87). Discontinuities were introduced in the maps whenever excessive distortions would have resulted from the flattening procedure. The recording sites and the myeloarchitectonic borders were projected orthogonal to the cortical surface onto layer IV, in each section, and then transferred to the flattened maps. In order to obtain the visuotopic maps of areas PO and POd for each animal, the location of the recording sites in the flattened maps and the corresponding coordinates of the receptive field centers were digitized, and maps for polar coordinates were obtained using the interpolation algorithm of Maunsell and Van Essen ('87). Linear scaling was used to interpolate eccentricity and polar angle values. Polar coordinates were interpolated between all possible pairs of recording sites to fill a grid of square bins (0.25 mm on a side). The array of bins containing the average value of the coordinate of each bin was used to draw isopolar and isoeccentric lines for each map, as is shown in Figure 11.

RESULTS

At least three myeloarchitectonically distinct regions, PO, POd, and POm, can be distinguished within cytoarchitectonic area OA (Von Bonin, '49) in the anterior wall of the parietooccipital sulcus and surrounding cortex (Fig. 1). Among these regions, at least PO and POd contain independent representations of the visual field. Area PO was identified using both myeloarchitecture and multiunit recordings in five animals. It corresponds to the heavily myelinated zone that borders V2 and extends into the anterior wall of the parietooccipital cleft. In each hemisphere area PO has a virtually complete, albeit complex, representation of the upper and lower contralateral visual quadrants (Fig. 2). The upper quadrant is represented medially in the precuneate gyrus. The lower quadrant is represented laterally in the anterior wall of the parietooccipital cleft and in the medial bank of the intraparietal sulcus.

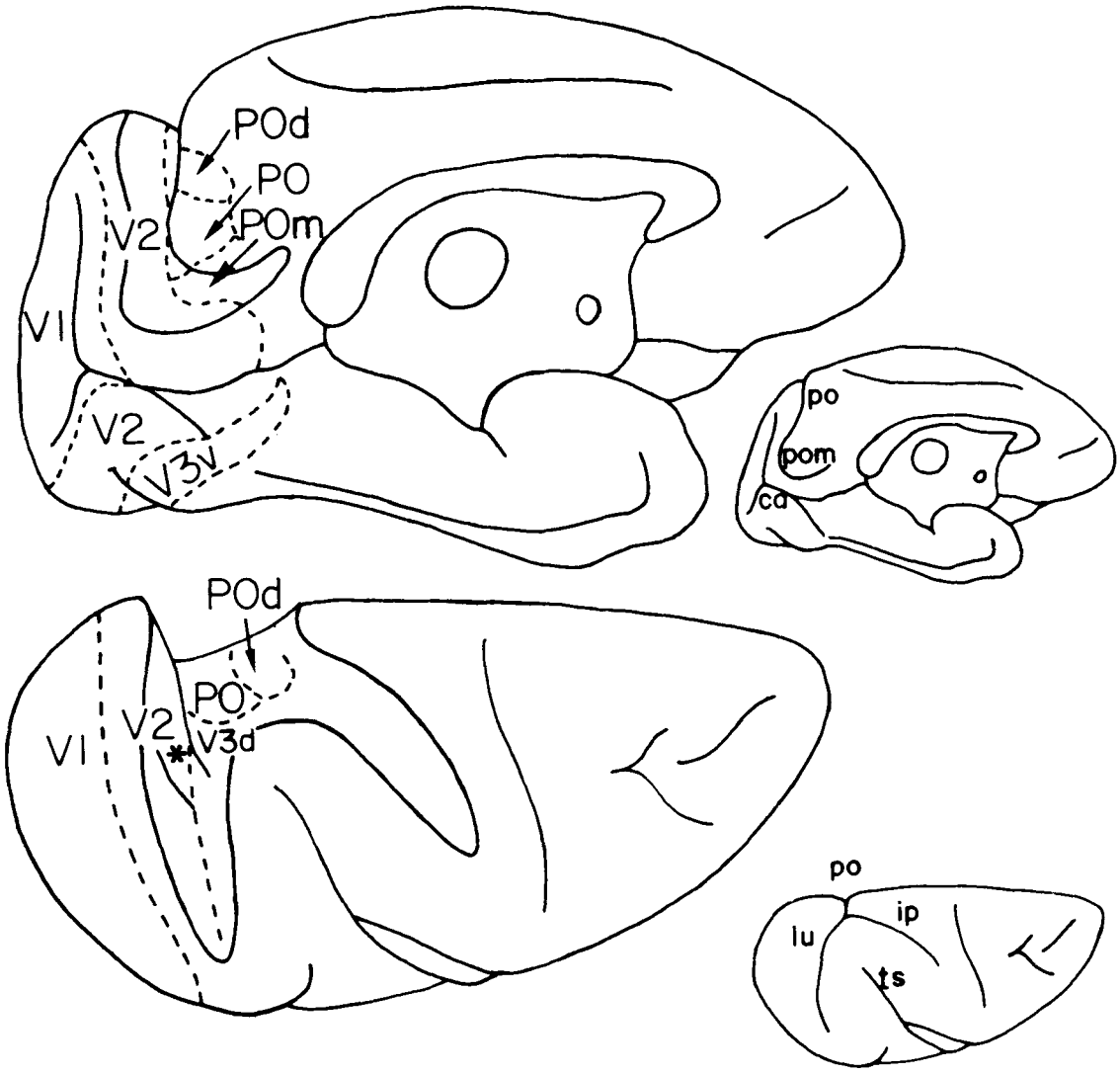

Fig. 1. Location of PO, POd, and surrounding areas. **Right:** Medial (upper) and dorsal (lower) views of the *Cebus* monkey brain. **Top left:** Medial view of the brain, with the parietooccipital sulcus partially opened. **Bottom left:** Dorsal view of the brain with lunate, intraparietal, and parietooccipital sulci partially opened. Dashed lines indicate the borders of PO, POd, and other visual areas. Asterisk, annectent gyrus.

The representation of the horizontal meridian runs dorsoventrally from the corner of the precuneate gyrus to the depth of the parietooccipital cleft. The vertical meridian is represented laterally and medially at the border of the area. The regularity in visuotopic organization of PO is apparent along the eccentric domain of the map (isopolar lines). The organization along the polar domain (isoeccentricity lines) is not simple. The location of the isoeccentricity lines varies from animal to animal, and these lines form complex patterns. In all animals only a rough separation of the central, intermediate, and peripheral representations is apparent. The representation of the peripheral 20–50° eccentricity is relatively more emphasized than the central representation. Area POd was identified in two animals. It was defined as an area dorsal to PO in the anterior wall of the parietooccipital cleft showing a complete representation of the contralateral visual field. Its myeloarchitecture is lighter and more stratified than that of PO. Its topographic organization is complex, and, similar to that of PO, it is simpler along the eccentric domain (isopolar lines) than along the polar one.

Myeloarchitecture

PO. The myeloarchitectonic pattern of PO shown in Figure 3 corresponds to the conjunct-striated pattern described by Sanides ('72). The infragranular layers of PO are heavily myelinated. The inner and outer bands of Baillarger are confluent. The layers above the outer band of Baillarger are pale and less myelinated than those in the adjacent cortex.

Myeloarchitectonic transitions between PO and the laterally and medially located areas are easily determined in coronal sections, and those with ventral and dorsal areas in parasagittal sections. In some animals the lateral portion of PO has a 1.5 mm wide myeloarchitectonic transitional

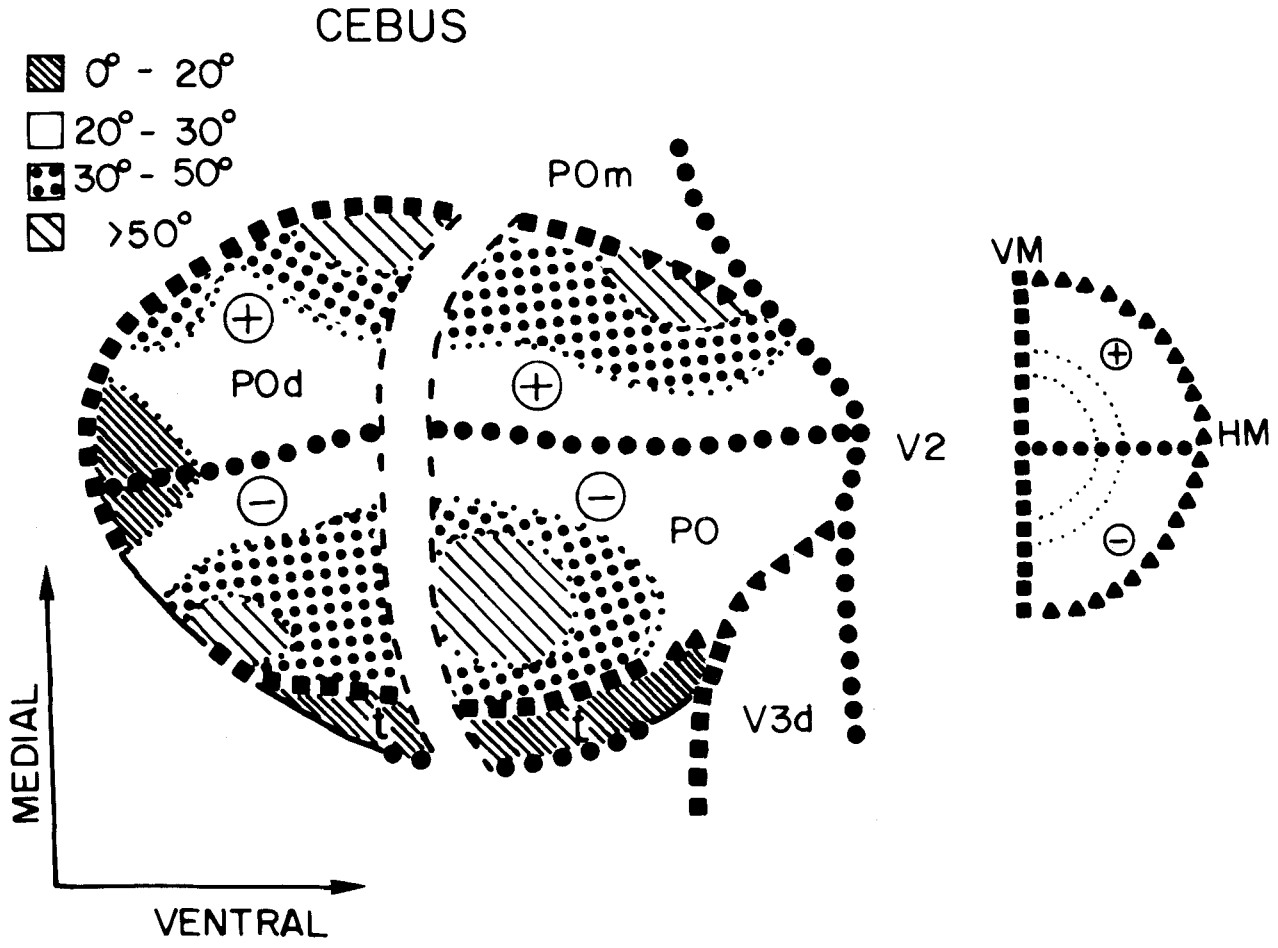

Fig. 2. Visual topography of PO and POd on a flattened reconstruction of the anterior bank of the parietooccipital sulcus. The squares indicate the vertical meridian (VM), the circles the horizontal meridian (HM), the triangles the periphery, and the dotted lines isoeccentricity lines. The dashed lines indicate the PO/POd myeloarchitectonic border. +, Upper quadrant; −, lower quadrant.

region, which borders area V3d. This transitional zone is less dense than the core of PO, but it is more myelinated than V3d. Based on topographic data, the representation of the visual field in this transitional zone complements that of the core of PO and hereafter shall be considered an integral part of PO. In other animals, no myeloarchitectonically transitional zone was observed. In these and other animals, the V3d/PO border was not clear in all sections.

POm. Area POm presents a more differentiated and less dense outer band of Baillarger than PO (Fig. 3). Posteriorly PO is bordered by V2, an area that has a homogeneous pattern of myelination in the lower layers (Rosa et al., '88), which is not as dense as that of PO. In addition, the outer band of Baillarger in V2 is less conspicuous and is less dense than that of either PO or POm. The border of PO with POm coincides with a decrease in myelination in the infragranular layers in POm.

POd. The dorsal border of PO with POd was determined in parasagittal sections (Fig. 4). POd is less myelinated than PO and has individualized inner and outer bands of Baillarger. The inner band gradually joins the white matter. The outer band is thinner than that of PO but well differentiated. A less myelinated area borders POd dorsally. This area has a stratified myeloarchitectonic pattern with a light outer band of Baillarger. This area may correspond to area PEc defined in *Macaca* by Pandya and Seltzer ('82).

Electrophysiological borders

The limits of PO and POd with their neighboring areas were determined either by abrupt changes in receptive field size or by reversals in the progression of receptive field centers recorded in sequential penetrations through the cortex. The large scatter in receptive field position and the complex topography of PO and POd severely strained the analysis of the topographical data. A combination of electrophysiological and myeloarchitectonic criteria described below were used in six animals.

Changes in the progression of receptive field centers mark the borders of PO and POd with the surrounding areas (Figs. 5–7). The border of PO and POm with V2 coincides with the representation of the horizontal meridian (Figs. 5, 6), while the border of PO with V3d coincides with the representation of the peripheral vertical meridian (Figs. 5, 6). A small invasion of the upper quadrant is sometimes observed at the V2/POm border (Figs. 5, 6). In addition, small changes in the receptive field size mark the border of PO (not illustrated) and POm (Figs. 5, 6) with V2 and V3d.

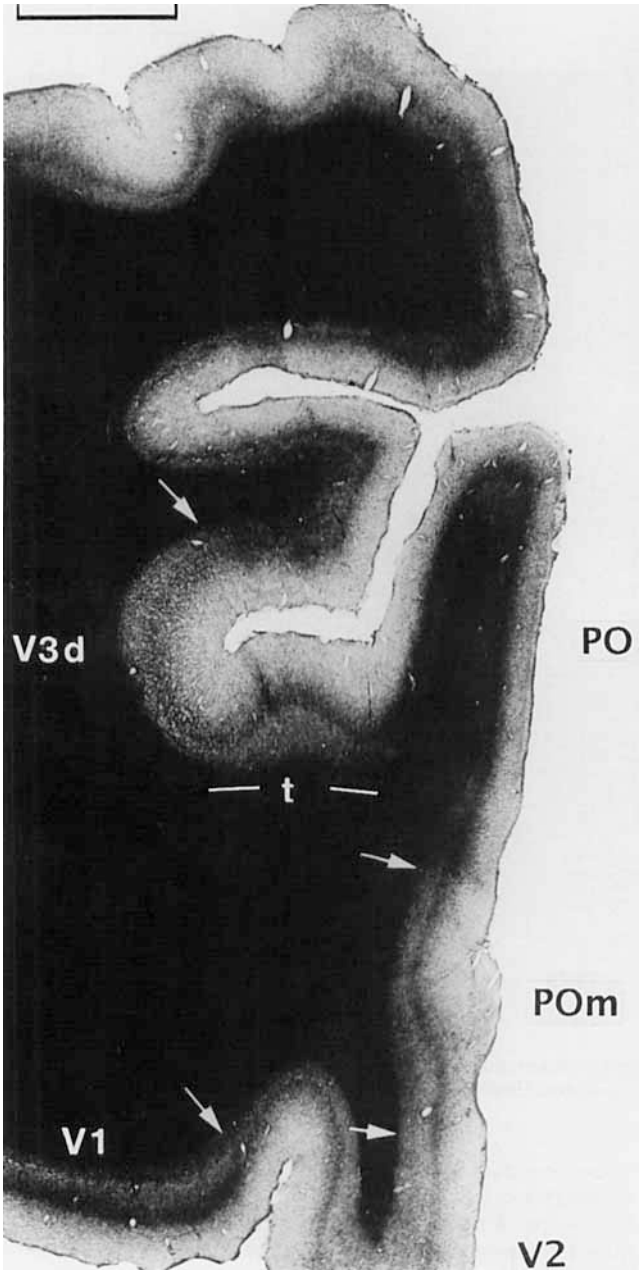

Fig. 3. Photomicrograph of a myelin-stained frontal-oblique section (same as in Fig. 6) showing the transitional zone (t) and the borders of PO, POm, and surrounding areas. Arrows point to myeloarchitectonic borders, bars point to myeloarchitectonic transitions. Scale bar = 2.0 mm.

Within PO, the border of the heavily myelinated region with the transitional myeloarchitectonic region corresponds to the representation of the vertical meridian (Figs. 5, 6). Subtle changes in the progression of receptive field centers at the intermediate portions of the visual field coincide with the myeloarchitectonic borders between PO and POm as well as between PO and POd (Figs. 5–7).

In addition, the border of PO with POd (Figs. 6, 7) coincides with a small change in receptive field size. The border between these two areas was drawn so as to preserve a virtually complete representation of the visual hemifield in each area. At this border, however, any discontinuity or reversal in receptive field progression cannot be distinguished from the intrinsic irregularities present in the visual maps of PO or POd. In Figure 7, for example, the discontinuity in the progression at the border of PO with POd (fields 6 and 10) does not differ from those located within area PO (for example, fields 10 and 11). Conversely, in the upper quadrant periphery (Fig. 8, section D), no clear discontinuity is observed at the border between these two areas. Although the variability of receptive field sizes precludes the definition of the PO/POd border based on field size, the receptive fields in PO tend to be smaller than those of POd. Because of irregular topography the precise location of the PO/POd border in each individual section had to be determined solely on myeloarchitectonic grounds. The myeloarchitecture of PO and POd, however, is very distinct, and it is always possible to draw the limit between these two areas. The electrophysiological PO/POd border, based on the overall topography, has always coincided with the myeloarchitectonic one.

The vertical meridian is represented at the dorsal border of POd with PEc. Beyond the border, the topography breaks down and a drastic change in receptive field size occurs. The visual receptive fields in PEc, whenever present, are much larger than those in POd.

The visual topography at the border of POd with POm is often noncongruent (Fig. 7, fields 31, 32). Close to this border, POd represents the upper vertical meridian, while, within POm, the lower periphery is represented (Fig. 7, fields 25–31 in POd and fields 32–33 in POm).

Visual topography of PO and POd

Figures 8–10 illustrate a series of oblique sections in animal PO-05 with recording sites in PO and POd and the corresponding receptive fields. The upper quadrant is represented medially and the lower quadrant laterally (see, e.g., Fig. 9, section E). As in all animals, a certain degree of overlap of receptive field centers is present at adjacent recording sites (see, e.g., Fig. 8, section B; Fig. 9, section C). However, trends in the representation become evident when analyzing sets of sequences. For instance, Figure 11 shows the locations of receptive field centers and recording sites on a flattened reconstruction of PO and POd from the same animal. In both areas receptive field centers recorded on medial lateral rows of penetrations progress from the upper to the lower visual quadrant in an organized fashion. However, a great deal of overlap is observed among receptive field centers belonging to different rows in the cortex. Nonetheless, receptive fields in PO and POd represent the same region in visual space, implying independent representations in the two areas. Similar results for animal PO-03 are illustrated in Figure 12.

Extensive overlap of receptive field centers occurs at recording sites located close to the PO/POd border, and this overlap does not differ from the intrinsic scatter observed within each area. However, we favor the separation of areas PO and POd inasmuch as we find support for this subdivision in the myeloarchitecture and in the pattern of connectivity of these areas (Colby et al., '88; Neuenschwander, '89; Sousa et al., '91).

An area of myeloarchitectonic transition designated as "t" in the figures, was found in two animals (PO–5 and PO–3) at the lateral portion of PO and POd (Figs. 5, 6). This area was considered as part of PO or POd inasmuch as it

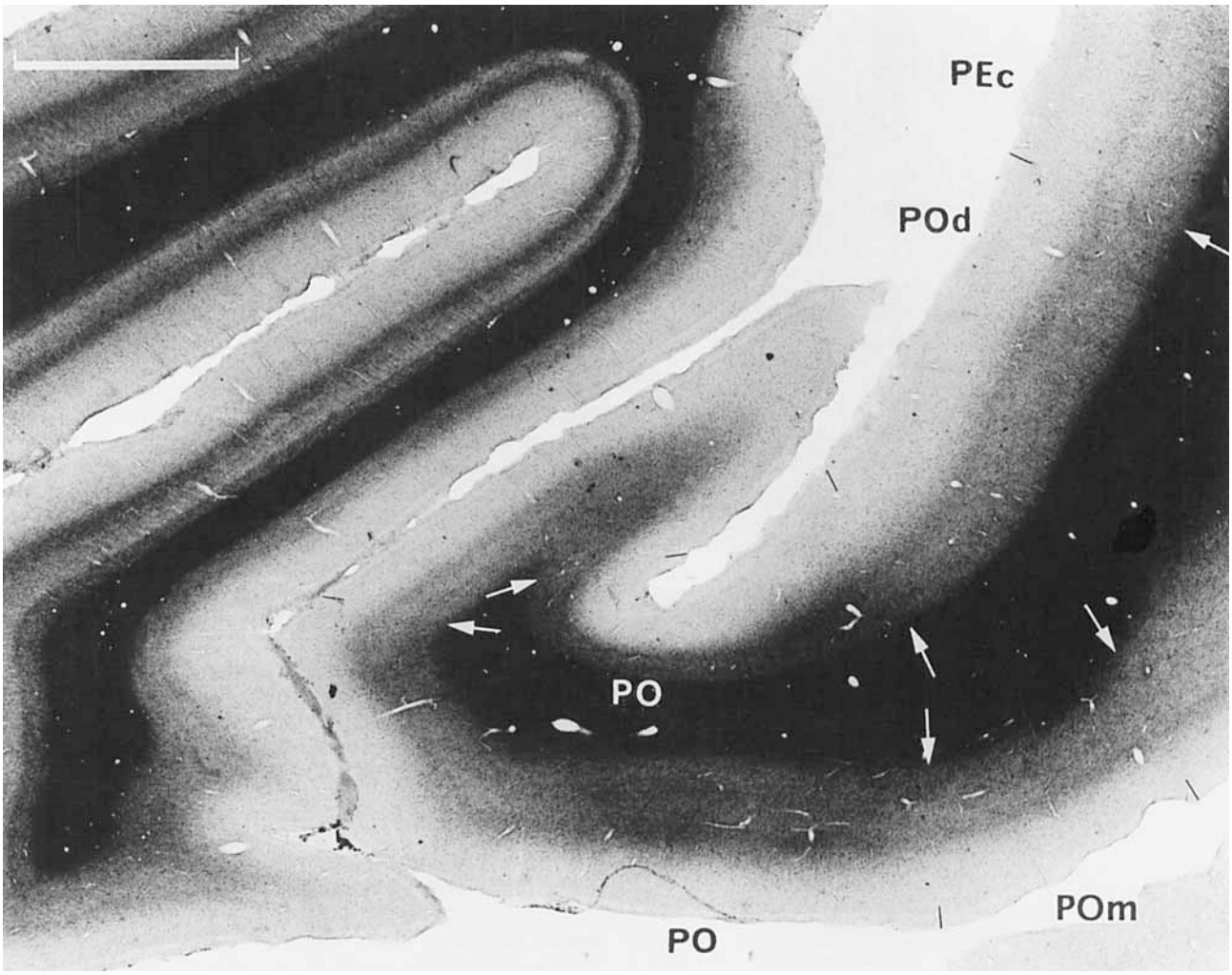

Fig. 4. Photomicrograph of a myelin-stained parasagittal section, showing the dorsal borders of PO and POd. White arrows and thin black lines point to myeloarchitectonic borders. Scale bar = 2.0 mm.

represents parts of the visual field not present in these areas (Figs. 11, 12).

Details of the visuotopic organization of PO and POd were evaluated in maps showing isoeccentric (Fig. 13, top) and isopolar (Fig. 13, bottom) lines drawn from arrays of interpolated coordinates, as described in Materials and Methods. In spite of individual variability (see below), a crude but consistent visuotopic organization was observed in all animals.

The degree of visuotopic orderliness and the existence of rerepresentations of sectors of the visual field in PO and POd were visualized by back-transforming onto the visual field a grid defined by an array of interpolated coordinates corresponding to equally spaced points in the cortex, following the procedure described by Maunsell and Van Essen ('87) (Fig. 14). As previously pointed out (Schwartz, '80; Van Essen et al., '84; Maunsell and Van Essen, '87; Fiorani et al., '89), a precisely organized cortical map would transform a square grid on the cortex onto an orderly cobweb pattern in the visual field. The back-transformed maps revealed individual variability in the degree of visuotopic orderliness in both PO and POd, with regular organization in the eccentric domain (isopolar lines) and a more irregular organization in the polar domain (isoeccentricity lines) in the cortex. A consistent bias towards rerepresentations of intermediate eccentricities could be observed in the back-transformed maps of animals PO-05, PO-03, and PO-02. These back-transformations suggest a tendency for greater representation of a sector of the visual field from 20–50° eccentricity. In area PO, no receptive field centers had eccentricity values $<5°$ (see, for example, Fig. 14). However, this result does not mean that the central field is not represented in PO, inasmuch as eccentric receptive fields do include the fovea (Fig. 16).

The topographic disorders in these maps are evident in the back-transformed maps (Fig. 14). The conclusion that PO is an area distinct from POd was based both on topographic and myeloarchitectonic analyses. In case PO-05, the multiplicity of central and peripheral representations shown in the map of eccentricities (Fig. 13) was considered as evidence for the existence of two distinct visual areas, which would contain virtually complete representations of the visual hemifield. Similar observations in other cases support this hypothesis. In case CB–11 (not

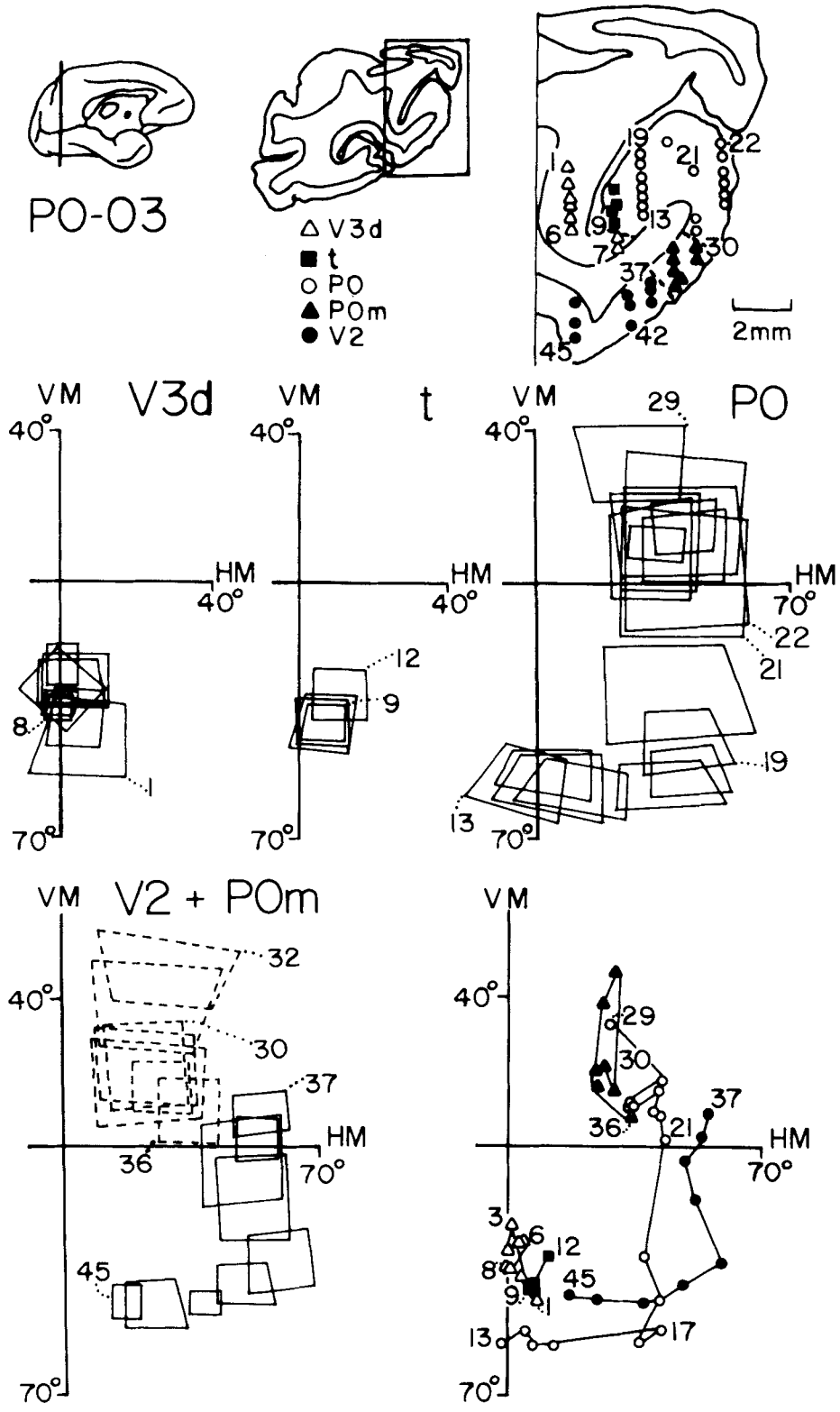

Fig. 5. Location of receptive fields in PO, transitional myeloarchitectonic area (t), and surrounding cortex, in animal PO-03 corresponding to recording sites shown in the enlarged view of the coronal section (top right), cut at the level indicated in the medial view of the brain (top left). Receptive fields and field centers are illustrated in cartesian representations of the visual field. Sequences of receptive field centers (bottom right) follow the projection of the recording sites on layer IV. Receptive fields of POm are drawn with dashed lines. For details see text.

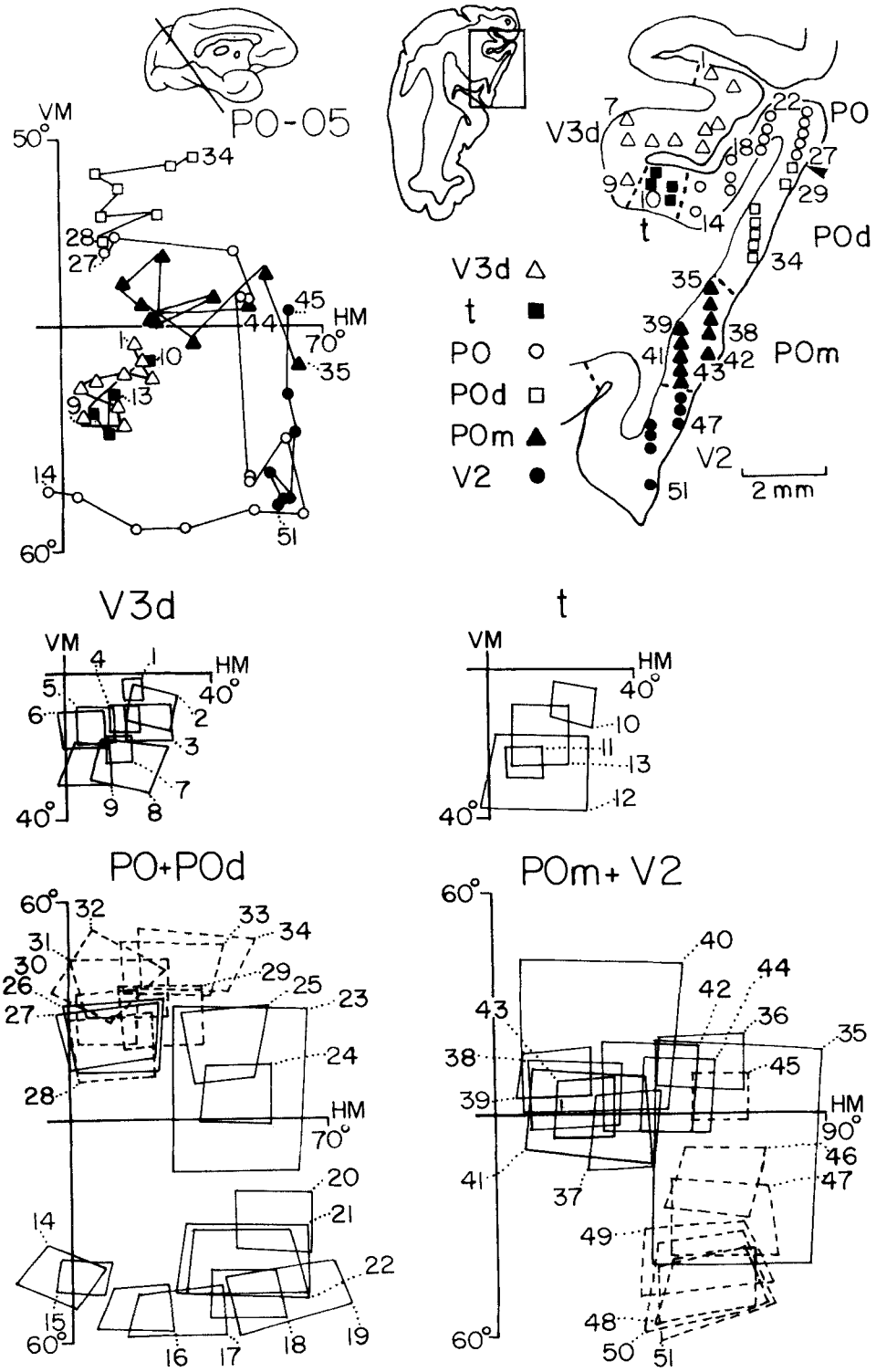

Fig. 6. Location of receptive fields in PO, POd, transitional area (t), and surrounding areas in animal PO-05, corresponding to recording sites shown in the enlarged view of the frontal-oblique section (top right), cut at the level indicated in the medial view of the brain (top left). Sequences of receptive field centers (middle left) follow the projection of the recording sites onto layer IV. Receptive fields in V2 and POd are drawn with dashed lines. Arrowhead points to the inferred PO/POd border.

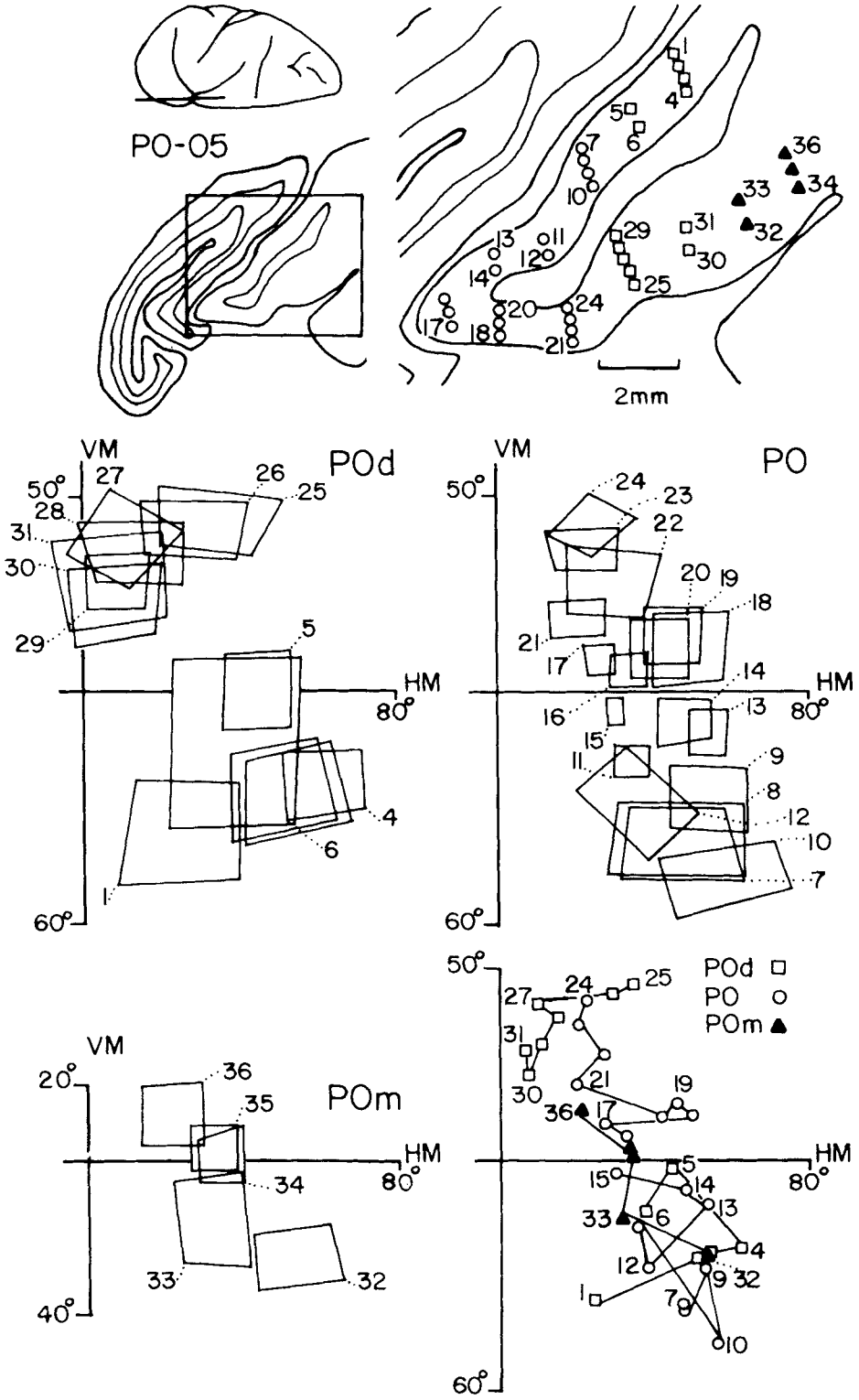

Fig. 7. Location of receptive fields in PO, POd, and POm in animal PO-05, corresponding to recording sites shown in the enlarged view of the parasagittal plane (top right). This plane is a reconstruction from the oblique sections illustrated in Figures 8–10, at the level illustrated in the dorsal view of the brain (top left). See also legend to Figure 6.

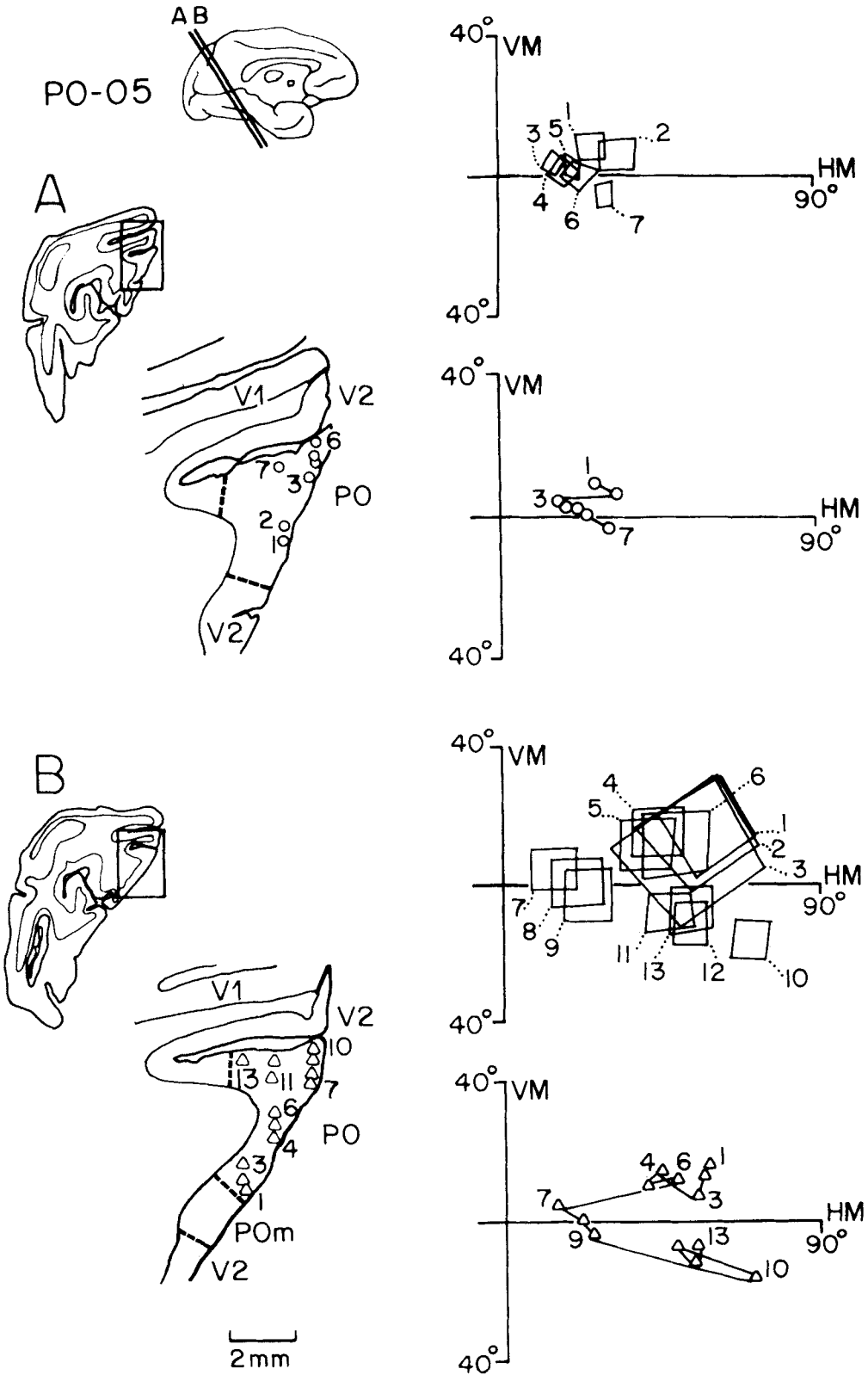

Fig. 8. Location of receptive fields (top right) and receptive-field centers (bottom right) in PO, corresponding to recording sites indicated in oblique frontal sections (**A,B**, bottom left) cut at the levels indicated in the medial view of the brain (top left). See also legend to Figure 6.

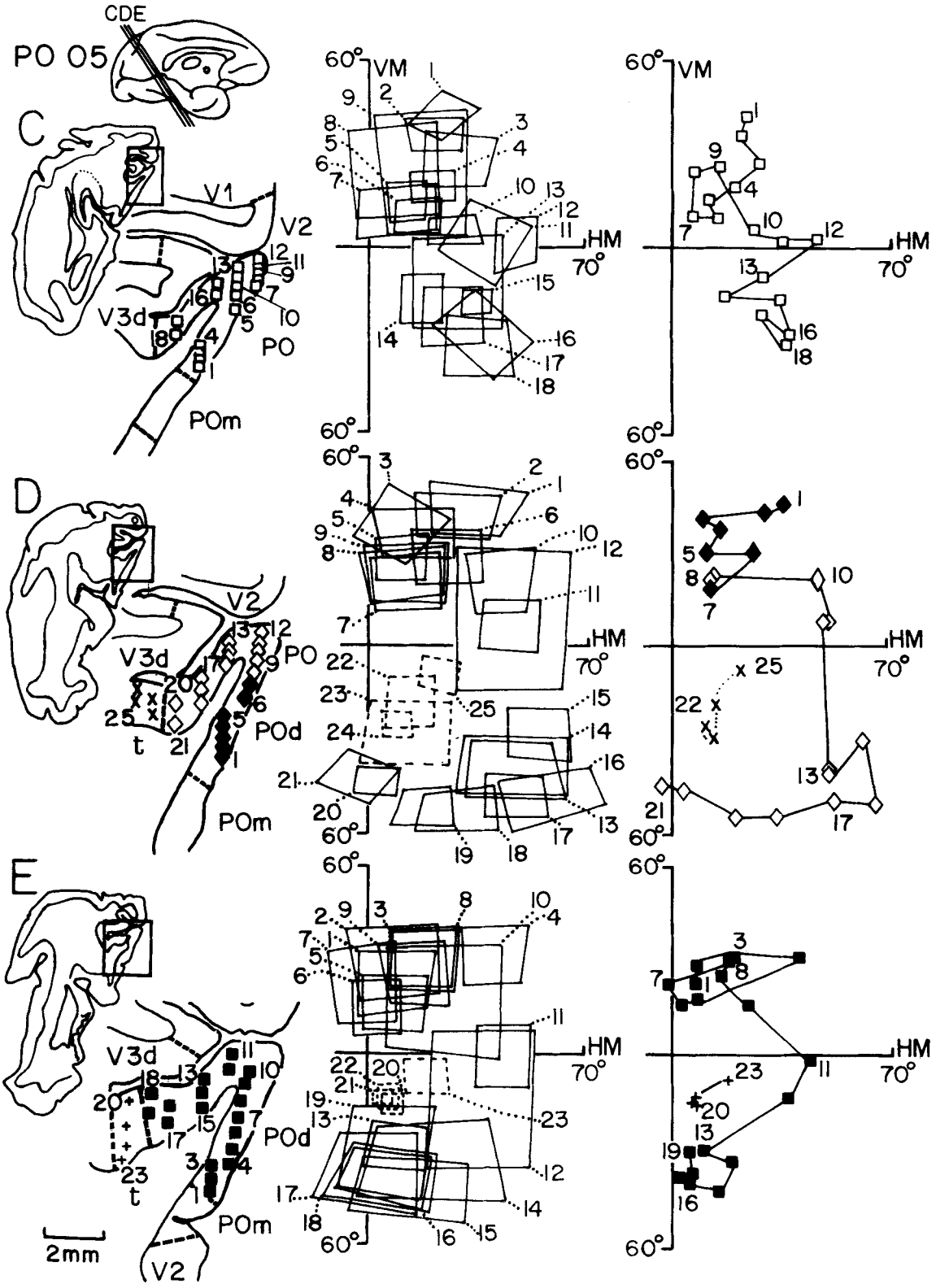

Fig. 9. Location of receptive fields (middle) and receptive field centers (right) in PO (open symbols), POd (solid symbols), and transitional zone t (×,+), corresponding to recording sites indicated in oblique frontal sections (**C–E**, left) cut at the levels indicated in the medial view of the brain (top left). See also legend to Figure 6.

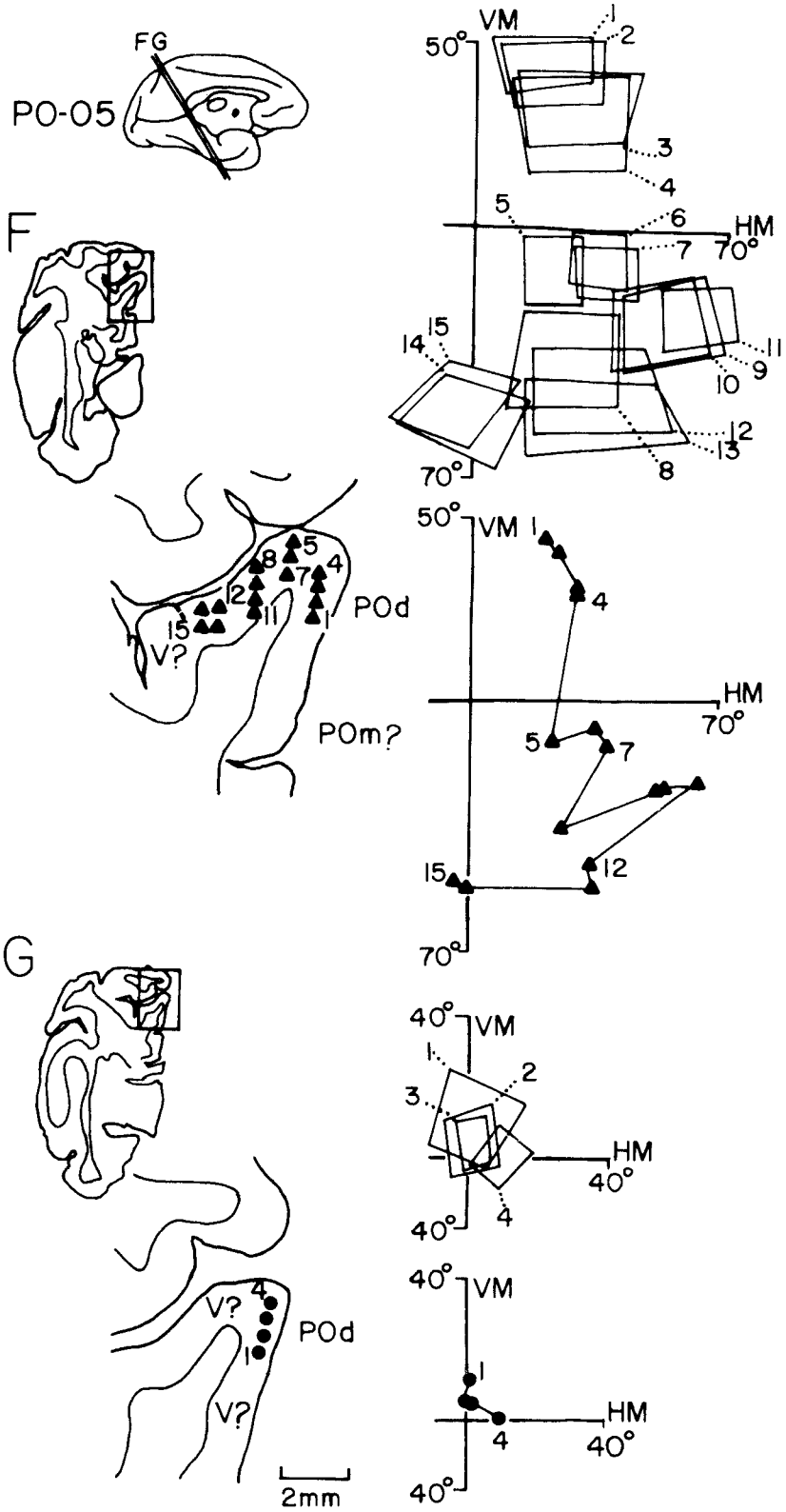

Fig. 10. Location of receptive fields (top right) and receptive field centers (bottom right) in POd corresponding to recording sites indicated in oblique frontal sections (**F,G,** bottom left) cut at the levels indicated in the medial view of the brain (top left). See also legend to Figure 6.

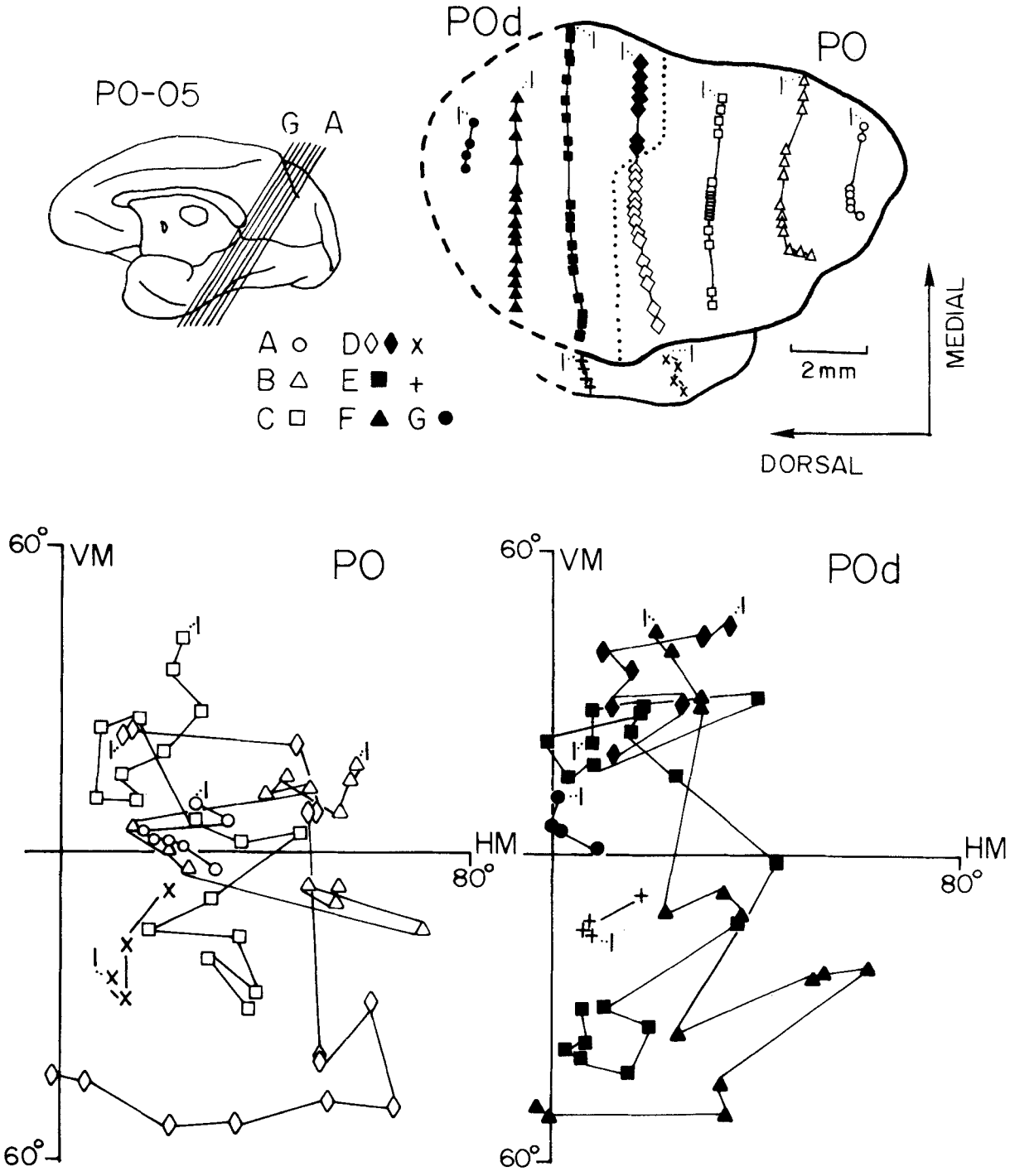

Fig. 11. Location of receptive field centers in PO (bottom left) and POd (bottom right) corresponding to recording sites indicated in the flattened reconstruction of the anterior bank of PO (top right) in animal PO-05. The oblique frontal planes (A–G) shown in the medial view of the brain (top left) correspond to those illustrated in Figures 8–10. In the flattened reconstruction, continuous lines indicate myeloarchitectonic borders, dashed lines electrophysiological borders, and dotted line the estimated electrophysiological border between PO and POd, which coincided with the myeloarchitectonic border.

illustrated), the visual hemifield is unquestionably represented both in PO and Pod, as defined on myeloarchitectonic grounds. Likewise, the dorsal portion labeled POd in case PO-03, (delimited by a dashed line) contains a rerepresentation of a portion of the visual field (sequences H and I in Fig. 12).

Cortical magnification factor

The cortical magnification factor (CMF), i.e., the ratio of the cortical distance between two recording sites, in millimeters, and the corresponding displacement of field centers, in degrees (Daniel and Whitteridge, '61), was determined

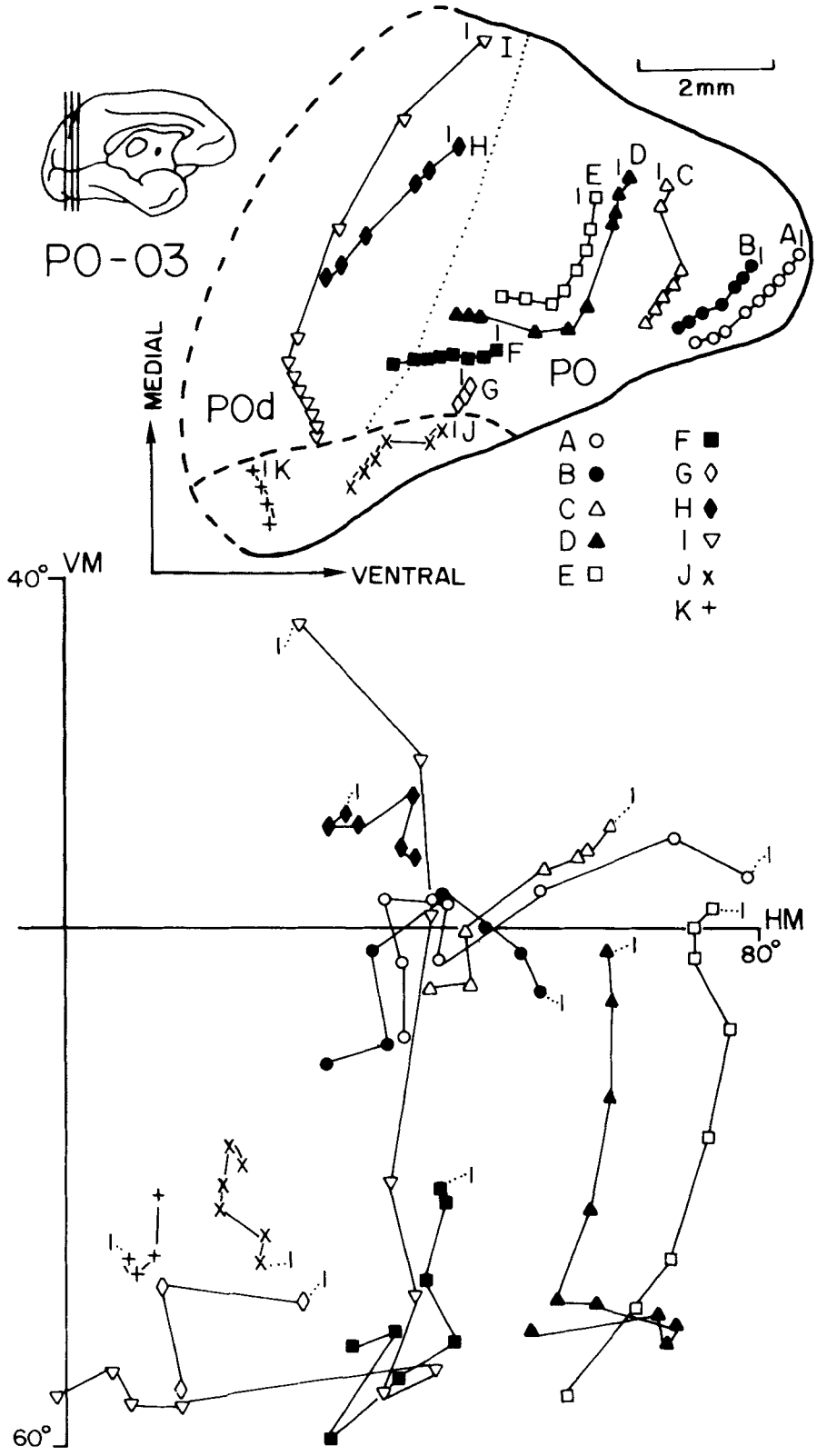

Fig. 12. Location of receptive field centers in PO, POd, and transitional zone in animal PO-03. In the flattened reconstruction, continuous lines indicate myeloarchitectonic borders, dashed lines electrophysiological borders, and dotted line the estimated electrophysiological border.

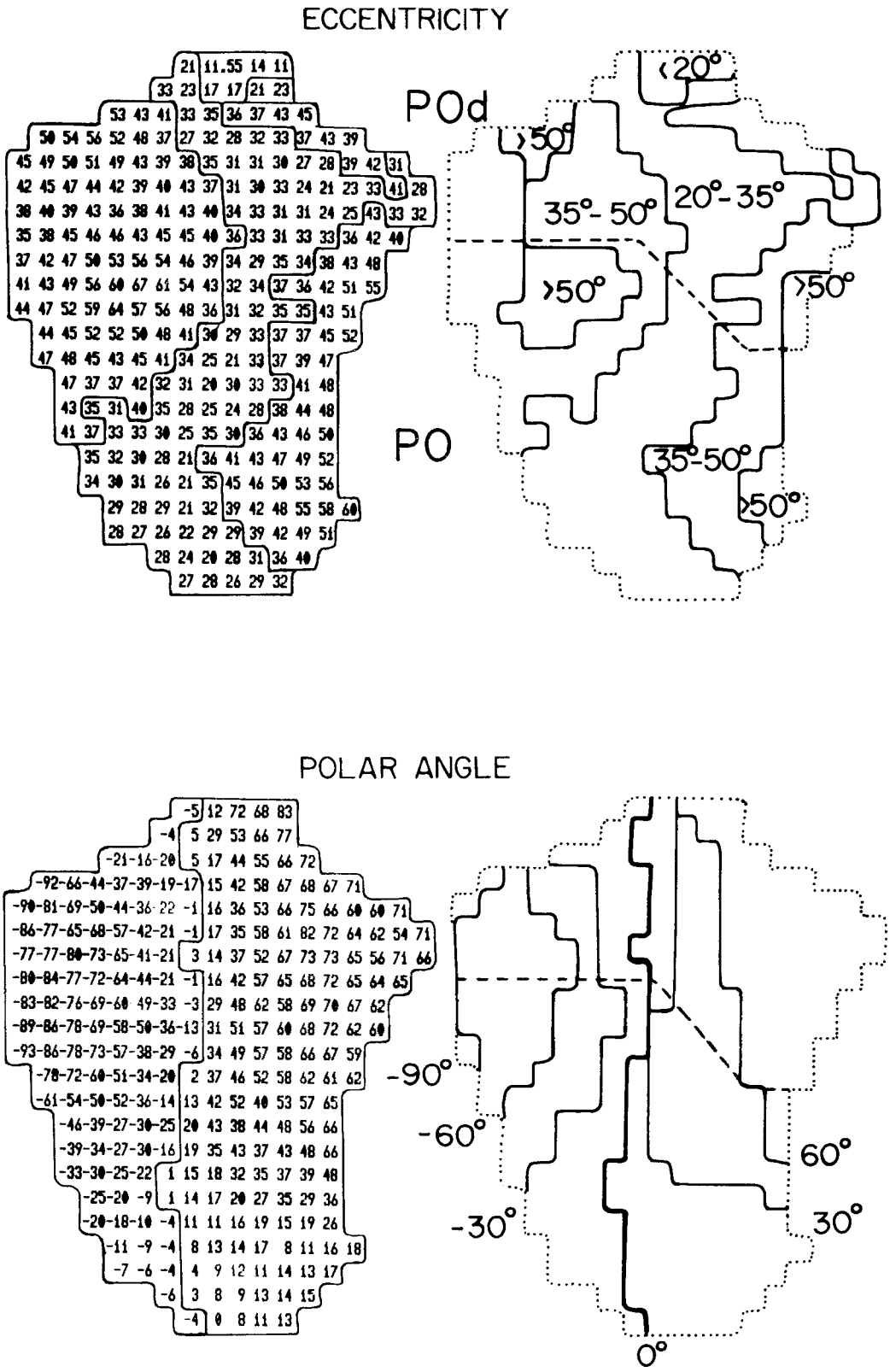

Fig. 13. Flattened maps of PO and POd showing interpolated eccentricity values (**top left**), derived isoeccentricity lines (**top right**), interpolated polar angle values (**bottom left**), and derived isopolar lines (**bottom right**). The maps containing isoeccentricity and isopolar lines were separated along the PO/POd border (dashed lines).

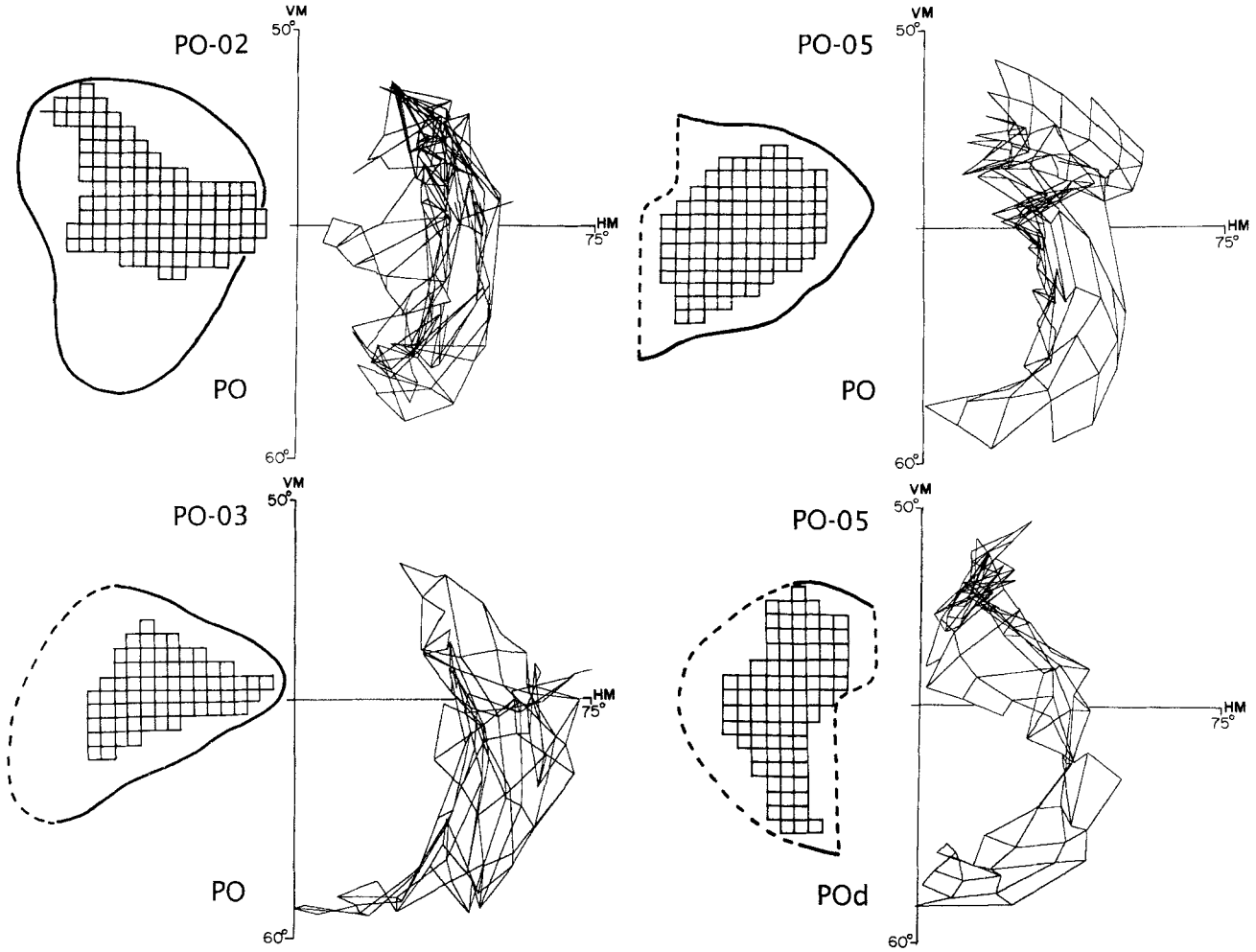

Fig. 14. Back-transformed maps for PO in animals PO-02 (**top left**), PO-03 (**bottom left**), and PO-05 (**top right**) and for POd in animal P0–05 (**bottom right**). Imaginary grids spaced by 0.5 mm on the cortical surface were back-projected onto the representation of the visual hemifield (right) at the corresponding values of the interpolated coordinates.

based on discrete measurements in PO and POd. The variation of CMF with eccentricity was evaluated with an automatic system, which calculates CMF by using all possible pairs of recording sites from digitized flattened maps of layer IV of PO and POd. Figure 15 (top middle) shows the plots of the cortical magnification factor as a function of eccentricity calculated for PO from data obtained in two animals.

The large dispersion of the data may reflect the scatter in receptive field positions and the complexity of the visual map of PO. Figure 15 (bottom) shows cortical magnification as a function of eccentricity for POd in animal PO-05.

Extent of the visual field in PO and POd

Area PO contains a representation of the contralateral visual field, which includes the binocular portion and a large part of the monocular crescent (Fig. 16, top and bottom left). The representation of a paracentral region of the lower quadrant was present in animals PO-03 and PO-05 at the laterally placed myeloarchitectonic transitional zone (t) bordering V3d. In animal PO-02, in which we were unable to find the transitional zone, this portion of the visual field was represented in the heavily myelinated portion of PO. The small emphasis on central field representation in PO may account for the "central sparing" in animals PO-03 and PO-05 (Fig. 14). Sampling differences in PO between animals PO-02 and the other two animals may account for the discrepancy in central field representation.

The extent of the visual field represented in POd (Fig. 16, bottom right), as determined in animal PO-05, is similar to that of PO (Fig. 16, bottom left). The interpolated maps of POd show, however, an even larger foveal representation for POd than that for PO. Thus we may infer that PO and POd contain a representation of the entire visual field. Although receptive field centers in both areas do not invade the ipsilateral visual field by $>4°$, some nasal boundaries extended 20° across the vertical meridian into the ipsilateral field.

Interanimal variability

The overall topography of PO, in which the upper quadrant is located medially and lower quadrant laterally, was present in all animals (Figs. 11, 12). The organization along the polar domain (isoeccentricity lines) was far more complex than that along the eccentric one (isopolar lines). A small representation of the central region (Fig. 13) and a greater representation of a sector of the visual field from 20° to 50° were also characteristics of PO in all animals.

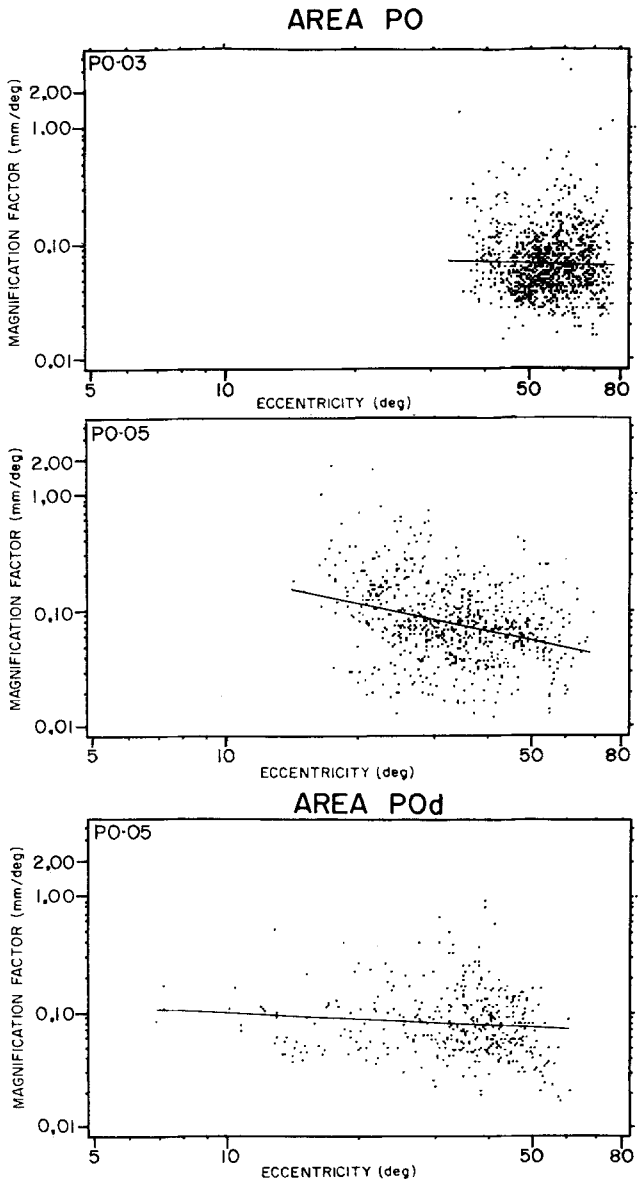

Fig. 15. Cortical magnification factor in PO (cases PO-03 and PO-05) and in POd (case PO-05) as a function of eccentricity. The power functions (lines) were fitted to the data by the method of least square.

These basic characteristics were accompanied by qualitative and quantitative differences in the organization of area PO from animal to animal. Variations were observed in the surface area, the shape and the relative emphasis of upper and lower quadrant representations (Fig. 14).

POd also proved to have some constancy with respect to location and overall mediolateral organization in PO-05 and PO-03. Nonetheless, POd varied in shape and surface area from animal to animal, but the paucity of data from PO-03 and CB–11 does not allow us to comment further on the variability of the organization of POd.

Receptive field size

The variation of multiunit receptive field size with eccentricity in PO and POd is shown in Figure 17. Different from other visual areas (Gattass et al.'86, '87; Rosa et al., '88; Fiorani et al., '89), the receptive field size in PO and POd, i.e. the square root of the receptive field area, does not change with increasing eccentricity. In order to compare this variation with that observed in other visual areas, a straight line was fit to the pooled data by the method of least squares. The slopes of these regression lines are not significantly different from zero, which suggests that field sizes both in PO and POd do not vary with eccentricity. The average receptive field size in PO is $17^{\circ 2}$ (SD = 7), while that of POd is $20^{\circ 2}$ (SD = 5).

Precision of the visual map

Because we did not make orthogonal penetrations through PO and POd, we were not able to determine receptive field scatter directly as proposed by Hubel and Wiesel ('74). In addition, the complexity of the visual maps of these areas, regular along only one dimension of the map, prevented us from using methods to determine scatter based on magnification factor (Fiorani et al., '89).

However, the comparison of the coordinates of field centers with the interpolated polar angles and eccentricities on the flattened surfaces of PO and POd allowed us to estimate the imprecision of the maps and thus the scatter. The imprecision was calculated by the vectorial difference of the coordinates of the receptive field centers from the ones predicted by the interpolating algorithm used to generate the bias free maps of polar angles and eccentricities. This measurement reflects the error of the location of the receptive field centers in the visual field in relation to the interpolated map, and it is similar in nature to the scatter calculated for MT by Gattass and Gross ('81). The ratio of scatter of receptive field size in PO and POd was shown to be smaller than one at various eccentricities (Fig. 18), indicating that the imprecision in these areas is smaller than the receptive field size and is constant across the visual field.

DISCUSSION

The location, topographic organization, and myeloarchitecture of area PO in *Cebus*, are similar to those of PO in the macaque (Covey et al., '82; Gattass et al., '87; Colby et al, '88). Even the surface area of PO is similar in these two species. Areal measurements of PO in three macaques (Colby et al., '88) revealed that PO is of about 79 mm^2, which corresponds to about 8% of the surface area of V1. This size is close to that of PO in *Cebus*, which has an area of 73 mm^2, equivalent to 7% of the surface area of V1. Interestingly, the surface areas of MT (Gattass and Gross, '81; Desimone and Ungerleider, '86; Fiorani et al., '89) as well as of V1 and V2 (Gattass et al., '81; Rosa et al., '88) are also similar in *Macaca* and *Cebus*. Thus *Cebus apella* and *Macaca fascicularis*, monkeys with similar body and brain sizes, also have cortical visual areas with equivalent sizes.

PO in the macaque was characterized in sections stained for myelin with Gallyas's method as a densely myelinated area with inner and outer bands of Baillarger separated by a paler band (Colby et al., '88). A plexus of tangential fibers in the infragranular layers distinguished PO from the neighboring V2 and V3. In *Cebus* we used the Heidenhain-Woelcke method for myelin. Nonetheless, we also observed a dense myelination and a rich plexus of tangential fibers in lower layers. These fibers according to Sanides ('72) are intracortical association fibers.

Covey and colleagues (Covey et al., '82; Gattass et al., '86) have described area PO in the macaque as a "complex,"

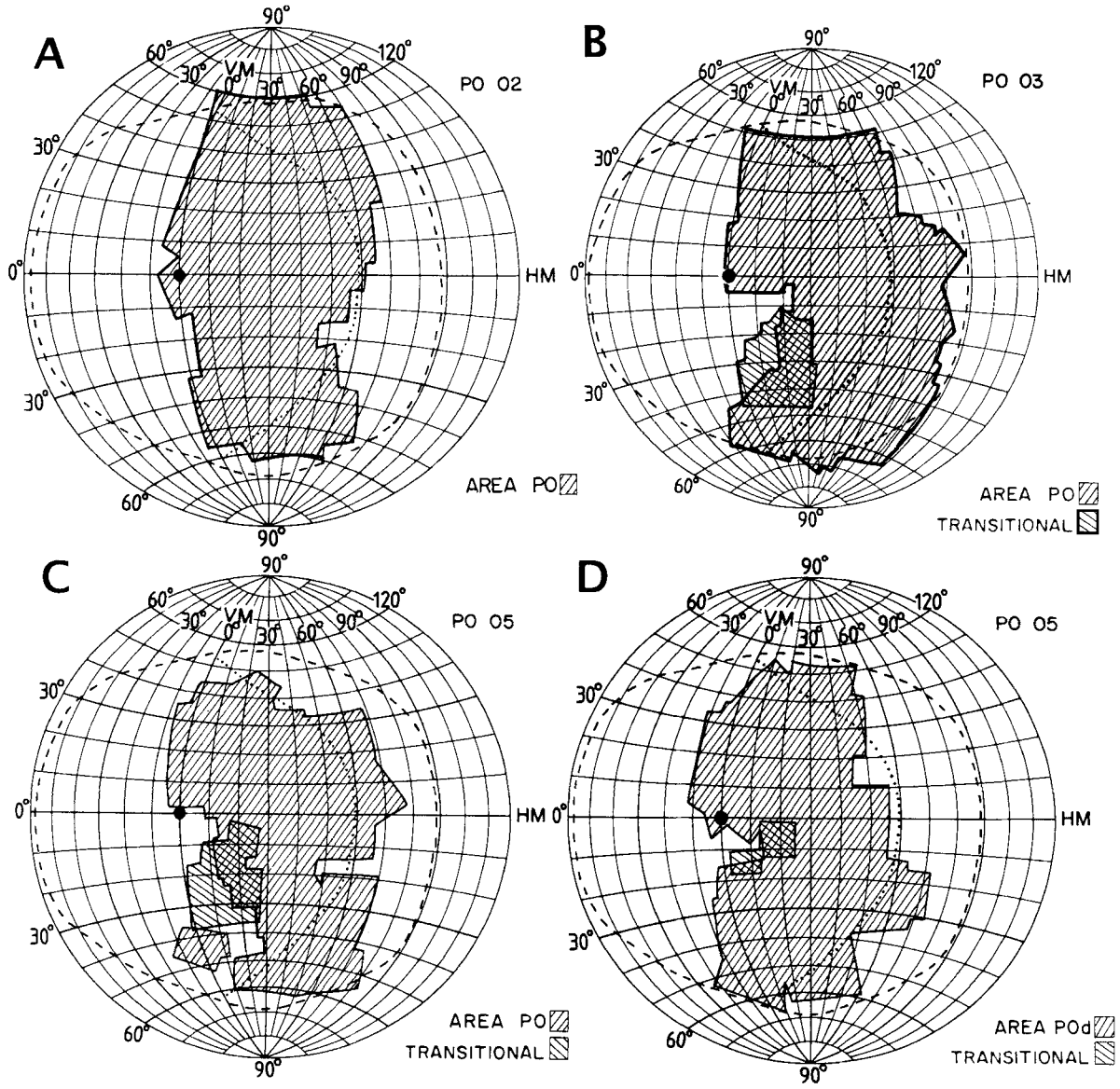

Fig. 16. Extent of the visual field represented in PO, POd, and the transitional zone. The shaded regions outline all receptive fields recorded in PO, POd, and transitional areas in animals PO-02, PO-03, and PO-05. Dashed line shows the extent of the monocular field of vision in three *Cebus* monkeys. The dotted line represents the temporal border of the binocular visual field, and the large dot the center of gaze.

which contains two central field representations: one in the lightly myelinated dorsal portion of PO and another in the heavily myelinated ventral portion of PO. Initially we chose a conservative interpretation of PO, in which we considered this region as one area "which could be further subdivided" (Gattass et al., '86). In our study in *Cebus,* the use of back-transformed maps to reveal rerepresentations of the visual hemifield and the pattern of myeloarchitecture has encouraged us to subdivide the "PO complex" into two visual areas: area PO and area POd. This interpretation finds support in more recent anatomical studies, which show that only the ventral portion of the "PO complex" as defined by Gattass et al. ('86), is connected with V1 in the macaque (Colby et al., '88) and in *Cebus* (Neuenschwander, '89; Sousa et al., '87, '91).

Projections from peripheral but not from central V1 to a region located in the medial wall of the hemisphere in a New World monkey, *Saimiri sciureus,* have been described (Martinez-Millán and Holländer, '75). The results in *Cebus* (Neuenschwander, '89) are comparable to those in *Saimiri* (Martinez-Millán and Holländer, '75) and in *Macaca* (Colby et al., '88). In *Cebus* PO has reciprocal connections with V1 (Sousa et al., '91). These results suggest homology of areas PO in these species of primates.

Covey et al. ('82) have proposed that area PO of the macaque could be homologous to area M of *Aotus* (Allman and Kaas, '76). This hypothesis was based on similarities in location and in topographic organization of areas PO and M. The visuotopic organization of area M and that of areas PO and POd are comparable only in general terms. On the other hand, the topographic maps of PO and POd in *Cebus* and in *Macaca* are coincident in several aspects, in spite of their complexity. In addition, this hypothesis does not find support for the connectivity or for the myeloarchitecture of

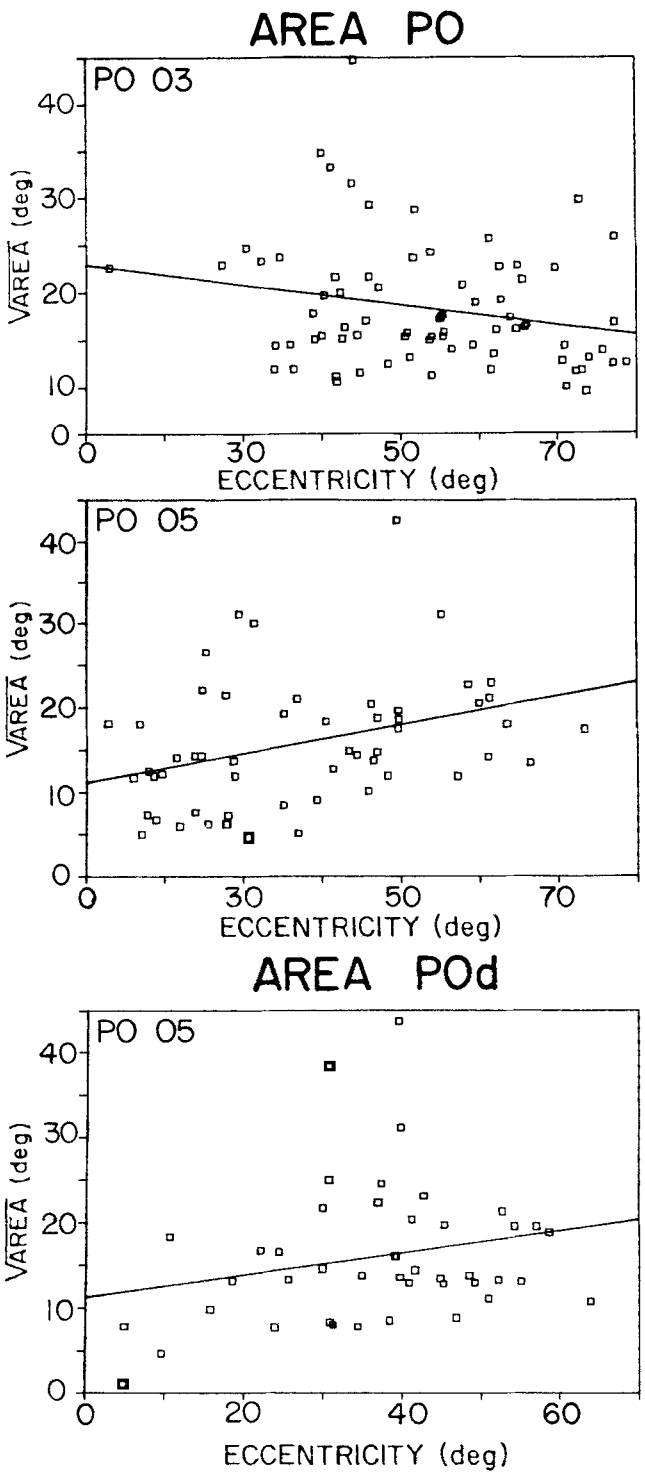

Fig. 17. Receptive field size as a function of eccentricity in PO and POd. Linear functions (lines) were fitted to the data by the method of least square.

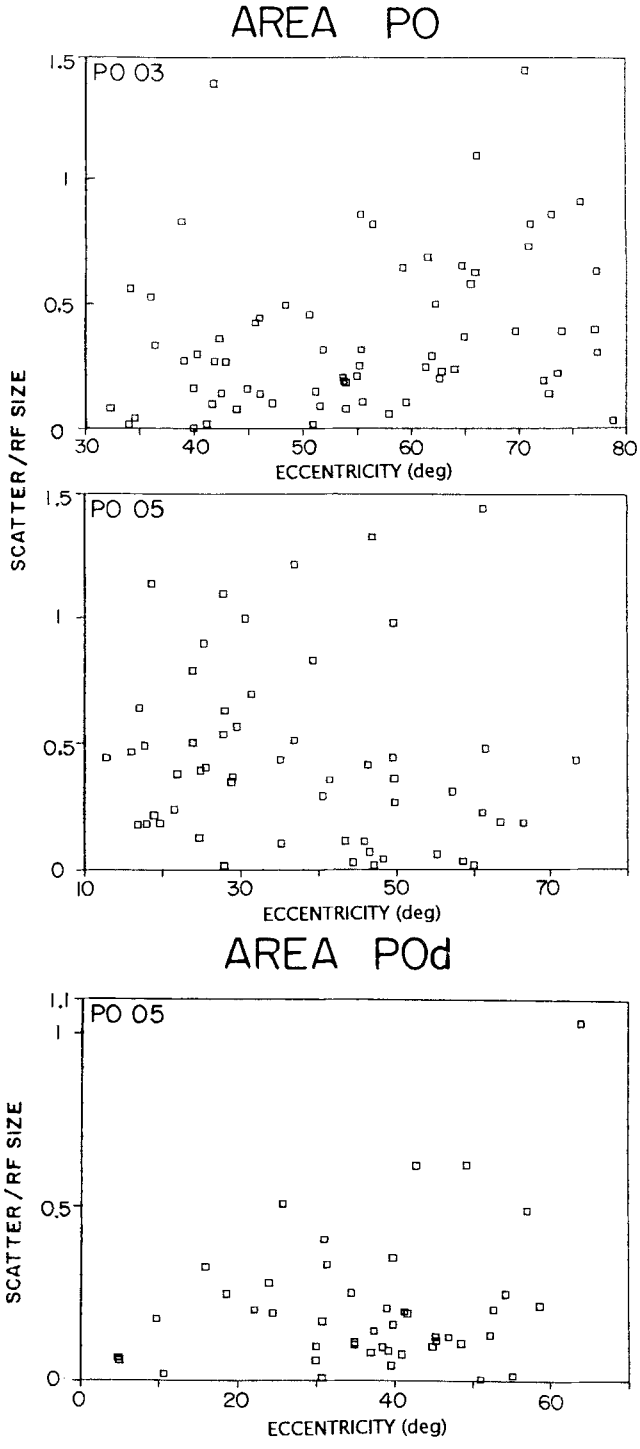

Fig. 18. Ratio of scatter in the interpolated map and receptive field position as a function of eccentricity in PO and POd.

these areas. While PO receives and sends projections to peripheral V1 (Colby et al., '88; Sousa et al., '91), area M does not. On the other hand, area DM is reciprocally connected with V1 (Grahan et al., '79; Lin et al., '82). In *Cebus* area PO has a dense myeloarchitectonic pattern, while area M in *Aotus* has a light one. A reasonable myeloarchitectonic correlation could be proposed between area PO of *Cebus* and area DM of *Aotus*. Thus we are left with two possible myeloarchitectonic homologies for area M of *Aotus*, areas POd or POm of *Cebus*.

Topographic organization

The visuotopic maps of PO and POd are complex representations of the visual hemifield. These representations are

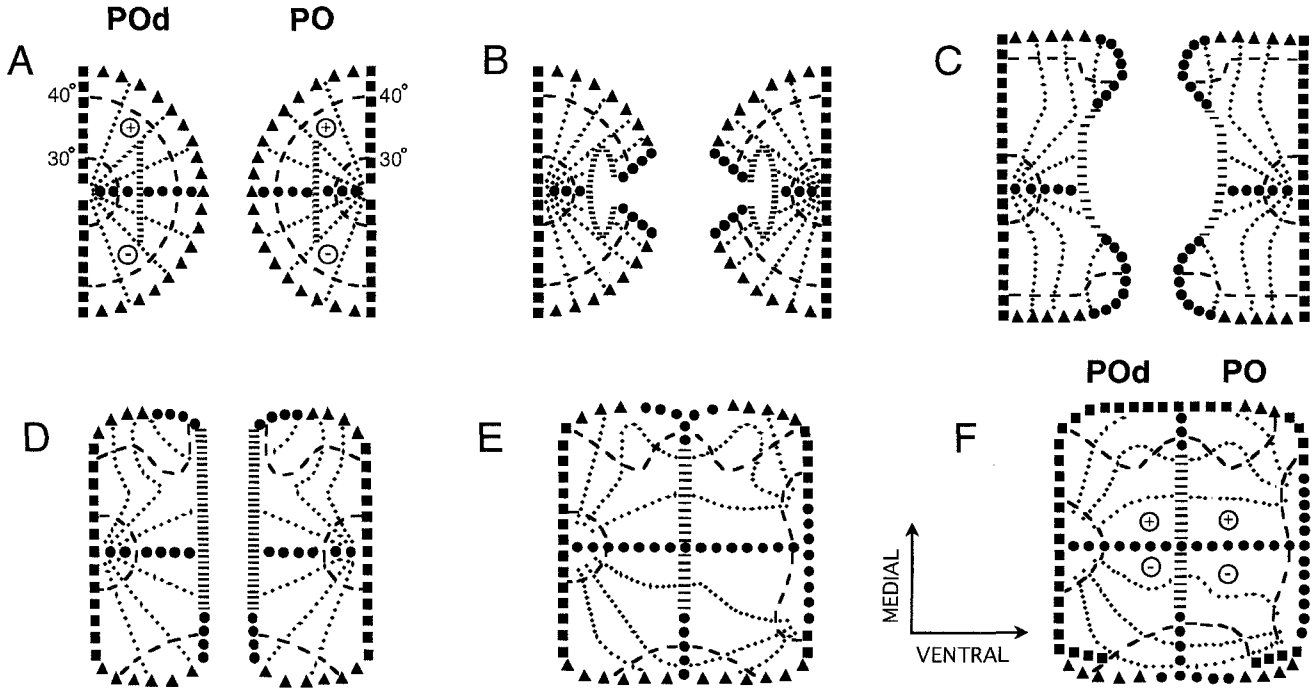

Fig. 19. Hypothetical transformations of the visual field to produce two independent and continuous maps of PO and POd, with complex arrangement along the isoeccentric domain and a simpler one along the isopolar domain. **A:** Two complete representations of the visual field facing each other. **B–F:** Steps of topological transformations leading to a complex map of PO (**right**) and POd (**left**) shown in F. Squares represent the vertical meridian; circles horizontal meridian; dashed lines isoeccentricity lines; dotted lines isopolar lines; triangles visual field periphery, and hatched lines intermediate portions of the visual field where discontinuities will occur.

not conformal to the retinal surface. Linear displacements in PO, such as those in penetrations of case PO-05 (Fig. 11), correspond to disorderly progressions in the visual field that do not follow spirals as one would expect from a nearly conformal representation of the visual field (Schwartz, '80).

Moreover, the visual maps of PO and POd have discontinuities and rerepresentations of portions of the visual field that appear to be different in nature from those previously observed in *Cebus* in areas V2 and MT (Rosa et al., '88; Fiorani et al., '89). These topographical irregularities in the visual maps of PO and POd are larger in the eccentric domain. They cannot be related simply to larger scatter in the maps, due to the increase of receptive field size with eccentricity as proposed for MT (Gattass and Gross, '81; Albright and Desimone, '87; Fiorani et al., '89), inasmuch as receptive field size in PO and POd is invariant with eccentricity.

The visual maps of PO and POd may be related to a specific arrangement of functional modules (as proposed at the end of this section) and/or may be related to topological constraints induced by its connections with neighboring areas. Area PO has congruent borders with V2 and V3, areas to which PO is connected (Colby et al., '88). Thus the distortions of the maps in PO and POd may also reflect transformations induced by its connectivity to neighboring areas. Figure 19 shows hypothetical transformations of the visual field representation to generate the complex maps of PO and POd. In Figure 19, two complete representations of the visual field facing each other at the visual field periphery (A) merge to form (B,C) two maps similar to those found in PO and POd. This unique organization of these areas with two congruent albeit complex maps suggests the possibility of cooperative interactions between these areas.

In addition the maps in PO and POd have a greater emphasis on peripheral representation than those of other prestriate areas such as V2 (Gattass et al., '81; Rosa et al., '88), V3 (Gattass et al., '88a,b), V4 (Gattass et al., '88a), and MT (Gattass and Gross, '81; Maunsell and Van Essen, '83; Desimone and Ungerleider, '86; Fiorani et al., '89). This "emphasis" is relative, inasmuch as cortical magnification in PO and POd appears to be constant throughout the visual field. Thus the emphasis on the periphery is a relative one compared to that of other cortical visual areas.

The cortical magnification factor (CMF) of PO in *Cebus* is comparable to that obtained for PO in the macaque (Gattass et al., '86). In the macaque, the cortical magnification factor varies from 0.3 to 1.7 mm/°, a range that includes the value found for *Cebus*. In the macaque, CMF also show a large dispersion for a given eccentricity. The scatter of CMF may also reflect local irregularities in the representation of the visual field in these areas.

No receptive field center was found at the upper vertical meridian in areas PO or POd. However, the more nasal receptive fields in this quadrant do include this meridian (Fig. 16). Similar observations in V2 (Gattass et al., '81), MT (Gattass and Gross, '81), V3, and V4 (Gattass et al., '88a,b) led to the conclusion that the vertical meridian beyond 5–10° eccentricity is represented by the nasal extent of receptive fields and not by their centers. This argument also applies for the representation of the fovea.

Point image size, i.e., the extent of the cortex driven by a punctual stimulus in the visual field (McIlwain, '76) has been proposed to be a relevant parameter for estimating the

size of the processing modules in the cortex. Dow et al. ('81) have estimated the point image size by the product of cortical magnification and aggregate field size (defined as the product of single unit receptive field size and scatter). These authors have shown that point image decreases with increasing eccentricity in V1. Gattass et al. ('87) have considered multiunit receptive field size to be related to both single unit field size and scatter. They have estimated the minimum point image size (MPIS) by the product of magnification and multiunit receptive field size. For PO and POd, we were unable to derive a clear MPIS function from the field size or magnification data. Thus we considered as an approximation of MPIS for PO and POd the product of the mean magnification factor and mean field size. The average MPIS for PO and POd is 1.7 mm. This value is larger than that obtained for both MT (Fiorani et al., '89) and the peripheral portion of V1 (Van Essen et al., '84; Gattass et al., '87).

Transitional zone. Areas PO and POd contain representations of virtually the entire visual field (Fig. 16). However, in two cases (PO-03 and PO-05), the superimposition of all receptive fields recorded in PO or POd did not include a paracentral portion of the lower quadrant. In these animals, the paracentral portion of the lower quadrant, coarsely complementing the representations of the visual field in PO and POd, was represented in transitional myeloarchitectonic regions. We hypothesize, therefore, that this transitional zone is part of areas PO and POd. Alternatively, we could also consider that the transitional zone could be part of a more lateral intraparietal area, not yet studied in *Cebus*. The transitional zone and the neighboring V3d have on average smaller receptive fields than PO or POd, possibly because they are more central than those of PO and POd.

Cortical streams of visual information processing. Anatomical and electrophysiological evidence in *Cebus* led us to suggest (Gattass et al. '90) a subdivision of the dorsal pathway defined by Ungerleider and Mishkin ('82) into two streams: a dorsomedial stream involving areas PO, POd, and PG and a dorsolateral one involving area MT, area MST, and the lateral intraparietal areas (Saito et al., '86; Goldman-Rakiç, '87; Colby et al., '88; Komatsu and Wurtz, '88; Neuenschwander, '89). We have proposed that the dorsomedial and dorsolateral streams may be involved in different aspects of spatial vision and motion (Gattass et al., '90).

The areas corresponding to the early stages in the dorsomedial pathway, such as PO and POd, contain representations of both the binocular and monocular visual fields. Thus a particularly interesting aspect of these areas is the virtual absence of receptive fields including the fovea, inasmuch as no receptive field centers were found below 5° of eccentricity in PO and only a few were found in POd. Note that receptive fields in area PG, a later stage of the dorsomedial pathway, often extend to the far periphery of the visual field and represent the fovea sparingly (Motter and Mountcastle, '81; Steinmetz et al., '87).

These differences in the emphasis on central vs. peripheral vision are likely to be related to the different roles performed by the ventral, dorsolateral, and dorsomedial streams (Gattass et al., '90). PO and POd, with a homogeneous representation of the visual field periphery, may provide the essential inputs mediating flow field perception during animal locomotion. In addition, stimulation of the visual field periphery was shown to dominate the perception of self movement, even when antagonistic moving images are presented at the center of gaze (Dichgans and Brandt, '74). Therefore, one could suggest that these areas with little central representation may be involved in visuomotor integration, oculomotor functions, and/or perception of global spatial relationships. An organization in the eccentric domain (with organized isopolar lines) may be important to compute trajectories of centrifugal saccades. Interestingly, PO, POd, and PG were shown to project to the pontine nuclei, which relay information to the part of the cerebellum involved in motor planning (Brodal, '78).

The homogeneous representation of the visual field and the constancy in field size with eccentricity in PO and POd are consistent with the characteristics of spatial vision throughout the visual field. These properties parallel the psychophysical ability to detect continuously moving targets, which is relatively invariant throughout the visual field (Bonnet, '77; Steinmetz et al., '87). The possible roles of areas PO and POd on flow field perception or on oculomotor programming should be tested in the near future.

The discovery of modules belonging to different streams of visual information processing within some cortical areas (Van Essen, '85; Zeki, et al., '89; Gattass et al., '90) have emphasized the segregated and distributed characteristic of information processing in the visual cortex. Topographical connections among different visual areas and modules led to the notion of cooperative processing of visual information in neighboring modules or areas. At present, we have no direct evidence regarding the functional significance of the observed order in the isopolar lines vs. disorder in the isoeccentric lines present in PO and POd. One may speculate, however, that centrifugal and centripetal organizations of directionality, such as those observed in area PG (Motter and Mountcastle, '81; Steinmetz et al., '87) and STP (Bruce et al., '81), demand interactions between neurons that analyze regions of space sharing a similar polar angle but with different eccentricities. Also, during forward egocentric motion, the angle of gaze is the center of the expanding flow field, which shows some constancy in the isopolar domain while presenting large changes in the isoeccentric domain. It may be that the intermixing of eccentricities of receptive fields in adjacent columns in PO and POd allows these interactions to occur by local circuits. Thus the visual maps of PO and POd may be the consequence of different computational strategies performed by these areas.

ACKNOWLEDGMENTS

We thank Drs. C.E. Rocha-Miranda, M.G.P. Rosa, and R. Desimone for helpful comments on the manuscript; Edil S. da Silva Filho for technical assistance; Virginia P.G.P. Rosa and Alexandre M. Saddi for the illustrations. We also thank Edna M.A. da Silva and Maria Tereza Monteiro for typing the manuscript and the Fundação Parque Zoológico de São Paulo for providing the animals used in these studies.

LITERATURE CITED

Albright, T.D., and R. Desimone (1987) Local precision of visuotopic organization in the middle temporal area(MT) of the macaque. Exp. Brain Res. *65*:582–592.

Allman, J.M., and J.H. Kaas (1971) A representation of the visual field in the caudal third of the middle temporal gyrus of the owl monkey (Aotus trivirgatus). Brain Res. *31*:85–105.

Allman, J.M., and J.H. Kaas (1974) The organization of the second visual area (V2) in the owl monkey: A second order transformation of the visual field. Brain Res. *76:*247–265.

Allman, J.M., and J.H. Kaas (1976) Representation of the visual field on the medial wall of occipital-parietal cortex in the owl monkey. Science *191:*572–575.

Bonnet, C. (1977) Visual motion detection models: Features and frequency filters. Perception *6:*491–500.

Boussaoud, D., R. Desimone, and L.G. Ungerleider (1991) Visual topography of area TEO in the macaque. J. Comp. Neurol. *306:*554–575.

Brodal, P. (1978) The corticopontine projection in the rhesus monkey: Origin and principles of organization. Brain *101:*251–283.

Bruce, C., R. Desimone, and C.G. Gross (1981) Visual properties of neurons in a polysensory area in superior temporal sulcus of macaque. J. Neurophysiol. *46:*369–384.

Colby, C. L., R. Gattass, C.R. Olson, and C.G. Gross (1988) Topographic organization of cortical afferents to extrastriate visual area PO in the macaque: A dual tracer study. J. Comp. Neurol. *269:*392–413.

Covey, E., R. Gattass, and C.G. Gross (1982) A new visual area in the parietooccipital sulcus of the macaque. Soc. Neurosci. Abstr. *8:*861.

Daniel, P.M., and D. Whitteridge (1961) The representation of the visual field on the cerebral cortex in the monkey. J. Physiol. (London) *159:*203–221.

Desimone, R., and L.G. Ungerleider (1986) Multiple visual areas in the caudal superior temporal sulcus of the macaque. J. Comp. Neurol. *246:*164–189.

Dichgans, J., and T.H. Brandt (1974) The psychophysics of visually induced perception of self-motion and tilt. In F.O. Schmitt and F.G. Worden (eds): The Neurosciences—Third Study Program, Vol. III. Cambridge, MA: MIT Press, pp. 123–129.

Dow, B.W., R.G. Snyder, R.G. Vautin, and R. Bauer (1981) Magnification factor and receptive field size in foveal striate cortex of the monkey. Exp. Brain Res. *44:*213–228.

Fiorani, M., Jr., R. Gattass, M.G.P. Rosa, and A.P.B. Sousa (1989) Visual area MT in the *Cebus* monkey: Location, visuotopic organization and variability. J. Comp. Neurol. *287:*98–118.

Freese, C.H., and J.R. Oppenheimer (1981) The capuchin monkeys, genus *Cebus*. In A.F. Coimbra-Filho and R.A. Mittermeier (eds): Ecology and Behaviour of Neotropical Primates, Vol. I. Rio de Janeiro: Academia Brasileira de Ciências, pp. 331–390.

Gattass, R., and C.G. Gross (1981) Visual topography of the striate projection zone in the posterior superior temporal sulcus (MT) of the macaque. J. Neurophysiol. *46:*621–638.

Gattass, R., C.G. Gross, and J.H. Sandell (1981) Visual topography of V2 in the macaque. J Comp. Neurol. *201:*519–539.

Gattass, R., A.P.B. Sousa, and E. Covey (1986) Cortical visual areas of the macaque: Possible substrates for pattern recognition mechanisms. Exp. Brain Res. (Suppl.) *11:*1–20.

Gattass, R., A.P.B. Sousa, and M.G.P. Rosa (1987) Visual topography of V1 in the *Cebus* monkey. J. Comp. Neurol. *259:*529–548.

Gattass, R., A.P.B. Sousa, and C.G. Gross (1988a) Visuotopic organization and extent of V3 and V4 of the macaque. J. Neurosci. *8:*1831–1845.

Gattass, R., A.P.B. Sousa, M.B.P. Rosa, and M.C.P. Piñon (1988b) Ventral V3 in the *Cebus* monkey: Visual topography and projections to V1. Soc. Neurosci. Abstr. *14:*202.

Gattass, R., M.G.P. Rosa, A.P.B. Sousa, M.C. Piñon, M.C., M. Fiorani Jr., and S. Neuenschwander (1990) Cortical streams of visual information processing in primates. Brazil. J. Med. Biol. Res. *23:*375–393.

Goldman-Rakiç, P.S. (1987) Circuitry of the prefrontal cortex and the regulation of behavior by representational memory. In F. Plum and V.B. Mountcastle (eds): Handbook of Physiology: The Nervous System V. Washington, DC: American Physiological Society, pp. 373–417.

Grahan, J., J. Wall, and J.H. Kaas (1979) Cortical projections of the medial wall visual area in the owl monkey, Aotus trivirgatus. Neurosci. Lett. *15:*109–114.

Hubel, D., and T.N. Wiesel (1974) Uniformity of monkey striate cortex: A parallel relationship between field size, scatter and magnification factor. J. Comp. Neurol. *158:*295–306.

Komatsu, H., and R.H. Wurtz (1988) Relation of cortical areas MT and MST to pursuit eye movements, I: Localization and visual properties of neurons. J. Neurophysiol. *60:*580–603.

Lin, C.S., R.E. Weller, and J.H. Kaas (1982) Cortical connections of striate cortex in owl monkeys. J. Comp. Neurol. *211:*165–176.

Martinez-Millán, M., and H. Holländer (1975) Cortico-cortical projections from striate cortex of the squirrel monkey (Saimiri sciureus). A radioautographic study. Brain Res. *83:*405–417.

Maunsell, J.H.R., and D.C. Van Essen (1983) The connections of the middle temporal visual area (MT) and their relationship to a cortical hierarchy in the macaque monkey. J. Neurosci. *3:*2563–2586.

Maunsell, J.H.R., and D.C. Van Essen (1987) Topographic organization of the middle temporal visual area in the macaque monkey: Representational biases and the relationship to callosal connections and myeloarchitectonic boundaries. J. Comp. Neurol. *266:*535–555.

McIlwain, J.L. (1976) Large receptive fields and spatial transformations in the visual system. Int. Rev. Physiology *10:*223–249.

Motter, B.C., and V.B. Mountcastle (1981) The functional properties of the light-sensitive neurons of the posterior parietal cortex studied in awaking monkeys: Foveal sparing and opponent vector organization. J. Neurosci. *1:*3–26.

Neuenschwander, S. (1989) Area visual parietoocipital (PO) do *Cebus apella*: Um estudo anatômico e eletrofisiológico. MS Thesis, Instituto de Biofísica Carlos Chagas Filho, UFRJ, 139 pp.

Neuenschwander, S., Gattass, R., Sousa, A.P.B., and M.C. Piñon (1990) The PO complex in Cebus monkey: Location and visuotopic organization. Abstr. 13th. European Conference on Visual Perception, Paris.

Pandya, D.N., and B. Seltzer (1982) Intrinsic connections and architectonics of the posterior parietal cortex in the rhesus monkey. J. Comp. Neurol. *204:*196–210.

Rosa, M.G.P., A.P.B. Sousa, and R. Gattass (1988) Representation of the visual field in the second visual area in the *Cebus* monkey. J. Comp. Neurol. *275:*326–345.

Saito, H., M. Yukie, K. Tanaka, K. Hikosaka, Y. Fukada, and E. Iwai (1986) Integration of direction signals of image motion in the superior temporal sulcus of the macaque monkey. J. Neurosci. *6:*145–157.

Sanides, F. (1972): Representation of the cerebral cortex and its areal lamination patterns. In G.H. Bourne (ed): The structure and function of nervous tissue, Vol. V. New York: Academic Press, pp. 329–453.

Schwartz, E.L. (1980) Spatial mapping in the primate sensory projection: Analytic structure and relevance to perception. Biol. Cybern. *25:*185–194.

Steinmetz, M.A., B.C. Motter, C.J. Duffy, and V.B. Mountcastle (1987) Functional properties of parietal visual neurons: Radial organization of directionalities within the visual field. J. Neurosci. *7:*177–191.

Sousa, A.P.B., R. Gattass, M.C. Piñon, and M.G.P. Rosa (1987) Cortical afferents to striate cortex in the *Cebus* monkey. Soc. Neurosci. Abstr. *13:*625.

Sousa, A.P.B., M.C. Piñon, R. Gattass, and M.G.P. Rosa (1991) Topographic organization of cortical input to striate cortex in *Cebus* monkey: A fluorescent tracer study. J. Comp. Neurol. *308:*665–682.

Ungerleider, L.G., and M. Mishkin (1982) Two cortical visual systems. In D.J. Ingle, M.A. Goodale and R.J.W. Mansfield (eds): Analysis of Visual Behavior. Cambridge, MA: MIT Press, pp. 549–586.

Van Essen, D.C. (1985) Functional organization of primate visual cortex. In E.G. Jones and A. Peters (eds): Cerebral Cortex, Vol. 3: Visual Cortex. New York: Plenum Press, pp. 259–329.

Van Essen, D.C., W.T. Newsome, and J.H.R. Maunsell (1984) The visual field representation in striate cortex of the macaque monkey: asymmetries, anisotropies and individual variability. Vision Res. *24:*429–448.

Von Bonin, G. (1949) The cerebral cortex of the *Cebus* monkey. J. Comp. Neurol. *69:*181–228.

Von Bonin, G., and P. Bailey (1947) The Neocortex of Macaca mulatta. Urbana, IL: University of Illinois Press.

Zeki, S. and S. Shipp (1989) The functional logic of cortical connections. Nature *335:*311–317.